Australian National University

Crawford School of Public Policy

CAMA

Centre for Applied Macroeconomic Analysis

Climate Shocks in Global Oil Markets: Time-Varying ENSO Transmission to WTI Spot and Futures Prices

CAMA Working Paper 56/2026
July 2026

Marco Gallegati
Polytechnic University of Marche, Italy

William Ginn
Labcorp, USA
Coburg University of Applied Sciences, Germany

Jamel Saadaoui
University of Paris 8, France
Centre for Applied Macroeconomic Analysis, ANU

Solomos Solomou
University of Cambridge, UK

Kun Tian
University of Kent, UK

Abstract

This paper studies whether global climate shocks are priced in global oil markets in a stable and homogeneous way. Using monthly data for 1983:03–2024:10, we estimate the response of real WTI spot and futures prices to phase-specific El Niño–Southern Oscillation (ENSO) anomalies. A Time-Varying Parameter Local Projection (TVP-LP) framework recovers horizon-specific coefficient paths, allowing transmission of the same measured anomaly to vary across historical market environments. ENSO transmission is asymmetric, time-varying, and spatially heterogeneous. El Niño anomalies lower real oil prices at six- to twelve-month horizons, whereas La Niña anomalies raise them. For futures prices, responses scaled to the sample means of the phase-specific absolute impulse variables—0.33◦C for El Niño and 0.39◦C for La Niña—imply declines of about 4.1–6.8 percent and increases of about 8.3–11.5 percent. Recent ENSO episodes generate more pronounced responses, consistent with stronger roles for climate information, futures-market expectations, inventories, and delayed supply-demand adjustment. Central-Pacific events, especially La Niña, are more inflationary than Eastern-Pacific events, which are typically muted or deflationary. The findings imply that climate shocks are macro-financial risk factors in global oil markets, with implications for inflation, energy prices, and international risk transmission.

Keywords

oil prices, oil futures, ENSO, climate risk, international transmission, time-varying local projections

JEL Classification

E31, F31, F36, G13, Q43, Q54

Address for correspondence:

(E) cama.admin@anu.edu.au

ISSN 2206-0332

Climate Shocks in Global Oil Markets: Time-Varying ENSO Transmission to WTI Spot and Futures Prices

Marco Gallegati[a], William Ginn[b], Jamel Saadaoui[c,d], Solomos Solomou[e], Kun Tian[f]

[a]*Polytechnic University of Marche, Italy.*
[b]*Labcorp, Sr. Economist / Data Scientist, Artificial Intelligence, USA and Coburg University of Applied Sciences, Germany.*
[c]*University of Paris 8, IEE, LED, 2 rue de la Liberté, Saint-Denis, France. Corresponding author.*
[d]*Australian National University, Centre for Applied Macroeconomic Analysis (CAMA), Australia.*
[e]*Faculty of Economics, University of Cambridge, Cambridge, UK.*
[f]*Kent Business School, University of Kent, UK.*

Abstract

This paper studies whether global climate shocks are priced in global oil markets in a stable and homogeneous way. Using monthly data for 1983:03–2024:10, we estimate the response of real WTI spot and futures prices to phase-specific El Niño–Southern Oscillation (ENSO) anomalies. A Time-Varying Parameter Local Projection (TVP-LP) framework recovers horizon-specific coefficient paths, allowing transmission of the same measured anomaly to vary across historical market environments. ENSO transmission is asymmetric, time-varying, and spatially heterogeneous. El Niño anomalies lower real oil prices at six- to twelve-month horizons, whereas La Niña anomalies raise them. For futures prices, responses scaled to the sample means of the phase-specific absolute impulse variables—0.33°C for El Niño and 0.39°C for La Niña—imply declines of about 4.1–6.8 percent and increases of about 8.3–11.5 percent. Recent ENSO episodes generate more pronounced responses, consistent with stronger roles for climate information, futures-market expectations, inventories, and delayed supply-demand adjustment. Central-Pacific events, especially La Niña, are more inflationary than Eastern-Pacific events, which are typically muted or deflationary. The findings imply that climate shocks are macro-financial risk factors in global oil markets, with implications for inflation, energy prices, and international risk transmission.

Keywords: Oil prices, Oil futures, ENSO, Climate risk, International transmission, Time-varying local projections
JEL: E31, F31, F36, G13, Q43, Q54

Email addresses: marco.gallegati@staff.univpm.it (Marco Gallegati), William.Ginn.OBA@said.oxford.edu (William Ginn), jamelsaadaoui@gmail.com (Jamel Saadaoui), ss19@cam.ac.uk (Solomos Solomou), kun_tian@outlook.com (Kun Tian)

Highlights

- ENSO shocks are priced asymmetrically in WTI spot and futures markets.
- El Niño lowers real oil prices; La Niña raises them at medium horizons.
- Recent ENSO episodes show stronger time-varying oil-price transmission.
- Oil futures embed ENSO information via expectations and inventories.
- CP and EP ENSO events transmit differently to oil prices.

1. Introduction

Global commodity markets increasingly price risks that originate outside the conventional macro-financial environment. Climate shocks are central to this process because they affect production, transportation, inventories, demand expectations, and risk premia. Oil markets provide a particularly important setting for studying this transmission. Oil is a central input into consumption, production, and global trade, and oil-price fluctuations propagate to inflation, trade balances, exchange rates, and monetary-policy trade-offs. The distinction between spot and futures prices is also important. WTI spot prices summarize conditions in the physical oil market, whereas WTI futures prices aggregate expectations about future demand, supply, inventories, financial conditions, and climate-related risks. This interpretation is consistent with evidence that crude-oil futures prices embed time-varying risk premia and forward-looking information about oil-market conditions (Hamilton and Wu, 2014). This makes oil futures a natural market in which to examine whether climate information is incorporated before the full physical effects of a climate shock are realized.

The El Niño–Southern Oscillation (ENSO) is among the most influential sources of global climate variability, affecting temperature, precipitation, drought, storms, agricultural output, energy demand, and supply chains (Ropelewski and Halpert, 1987; Rosenzweig et al., 2001; McPhaden et al., 2006; Dai, 2013; Brönnimann et al., 2007). ENSO is also useful for identification. Sea-surface-temperature anomalies in the tropical Pacific originate from ocean–atmosphere dynamics and are plausibly predetermined with respect to contemporaneous oil-price innovations. This external source of climate variation allows us to study how global climate shocks are transmitted to dollar-denominated oil spot and futures markets after conditioning on world demand, oil supply, and exchange-rate conditions.

Existing research shows that ENSO has important macroeconomic and commodity-market consequences. Dufrénot et al. (2024) show that El Niño tends to support output with limited inflationary effects relative to La Niña. Ginn (2025) further shows that La Niña steepens the Phillips Curve and generates stronger and more persistent inflationary effects than El Niño. Atems and Sardar (2021) demonstrate that the growth effects of El Niño and La Niña depend on local weather conditions. Ubilava (2017) identifies asymmetric ENSO effects in wheat price dynamics, while Dufrénot et al. (2026) shows that climate change alters the frequency and intensity of ENSO events, amplifying commodity-price volatility and macroeconomic vulnerability. The broader literature also points to phase asymmetries. La Niña episodes are often associated with higher food and agricultural commodity prices because they reduce yields, deplete inventories, and generate supply pressures (Iizumi et al., 2014; Gutierrez, 2017; Ubilava, 2012; Bastianin et al., 2018; Ab Rahman et al., 2013). These asymmetries matter for macro-financial analysis because commodity-price movements can transmit climate shocks to inflation and international relative prices.

The evidence on ENSO and oil prices remains mixed. Early studies largely focused on non-oil commodities. For example, Brunner (2002) finds that a one-standard-deviation El Niño shock increased non-oil commodity prices by 3.5 to 4 percentage points, while Laosuthi and Selover (2007) reports insignificant El Niño effects for most commodities. More recent work has considered oil prices, but the conclusions differ. Cashin et al. (2017), using a GVAR framework, finds that El Niño events generate short-term increases in oil prices through higher demand from major industrialized economies, whereas Solomou and Tian (2025) reports negative effects of El Niño shocks on oil prices. Evidence from energy markets suggests that the mechanisms are likely to be heterogeneous: Changnon (1999) links El Niño to lower heating-oil demand and prices, while Cruz and Krausmann (2013) emphasizes the vulnerability of oil production to extreme weather events. Multi-scale evidence reinforces this instability. Qin et al. (2020) finds a time- and frequency-dependent relationship between El Niño and oil prices, and Dufrénot et al. (2026) documents asymmetric effects across ENSO regimes and energy commodities.

The relevant empirical question is therefore not only whether ENSO affects oil prices on average, but whether the same physical anomaly is transmitted differently across oil-market environments. A constant-parameter local projection compresses the ENSO–oil-price relationship into a full-sample average response at each horizon. By contrast, the TVP-LP estimator of Inoue et al. (2024) recovers horizon-specific coefficient paths, allowing the response to depend on the calendar date at which the ENSO anomaly occurs. This distinction is central to the paper. An ENSO anomaly during the major late-1990s episode and an ENSO anomaly after 2015 are measured with the same phase-specific sea surface temperature (SST) variable, but their oil-price effects may differ because climate monitoring, information processing, futures-market pricing, inventories, supply-chain exposure, and oil-market structure have evolved over time.

The quantification follows directly from the construction of the ENSO variables. The El Niño and La Niña regressors are phase-specific absolute Niño 3.4 SST anomalies measured in degrees Celsius. The estimated coefficients are therefore dynamic multipliers for a one-degree Celsius increase in the corresponding phase-specific anomaly. Since the dependent variables are log real WTI prices, a coefficient $\hat{\beta}$ corresponds approximately to a percentage response of $100\hat{\beta}$ and exactly to $100[\exp(\hat{\beta}) - 1]$. For futures prices, the baseline LP estimates at horizons 6–12 imply El Niño coefficients ranging from -0.213 to -0.128 log points, corresponding to exact price declines of 12.0–19.2 percent. The corresponding La Niña coefficients range from 0.205 to 0.280 log points, corresponding to exact price increases of 22.8–32.3 percent. Scaling these responses to the sample means of the phase-specific absolute impulse variables, 0.33°C for El Niño and 0.39°C for La Niña, gives declines of about 4.1% to 6.8% and increases of about 8.3% to 11.5%, respectively.

The paper makes three contributions to the literature on international macro-finance, climate risk, and commodity markets. First, it shows that ENSO shocks are not homogeneous climate disturbances: El Niño and La Niña have opposite effects on real oil prices. Second, it provides evidence of time-varying climate-risk transmission. The same measured SST anomaly has different oil-price effects depending on when it occurs, with recent ENSO episodes producing stronger responses than earlier episodes. Third, it shows that spatial ENSO diversity matters for oil markets. Central-Pacific and Eastern-Pacific ENSO events transmit differently, implying that standard ENSO measures can obscure economically meaningful heterogeneity. Together, these results show that the market impact of ENSO depends on the interaction between the physical climate anomaly and the historical market environment through which it is priced.

These findings have international macro-financial relevance. ENSO-induced oil-price movements can generate cost-push inflation, affect real income and production costs, and complicate monetary-policy responses to energy-price shocks (Bernanke et al., 1997). They can also interact with the exchange-rate channel because oil prices are dollar denominated and global oil-market conditions are filtered through currency movements. This link is central to the international finance literature: oil prices, exchange rates, and interest rates are jointly connected in international commodity markets (Kilian and Zhou, 2022), while the oil-price–exchange-rate relationship can be empirically unstable and sensitive to the frequency and horizon under consideration (Ferraro et al., 2015). Fiscal authorities may respond to oil-price surges through fuel subsidies, which remain widespread and impose substantial fiscal costs (e.g., Coady et al., 2017; Balke et al., 2015; Clements et al., 2013). The results therefore speak to a broader question in international money and finance: how global non-financial shocks become priced in internationally traded assets and transmitted to inflation, exchange rates, and macroeconomic policy.

The remainder of the paper is structured as follows: Section 2 summarizes the data; Section 3 describes the methodology; Section 4 presents the empirical results; and Section 5 concludes.

2. Data

2.1. Global ENSO Climate Patterns

ENSO relates to cyclical, environmental conditions that occur across the equatorial Pacific Ocean. Changes to ENSO are due to natural interactions between sea surface temperature, rainfall, air pressure, atmospheric and oceanic circulation. The effects of ENSO, commonly called "teleconnections", emphasize that changing conditions can have a profound effect on global climate, which can in turn directly affect people's livelihoods (e.g., Barlow et al., 2001, Diaz et al., 2001, Alexander et al., 2002).

When a major El Niño occurs, warm SST anomalies in the tropical Pacific are associated with anomalous heat release from the ocean to the atmosphere, contributing to higher global mean temperatures. During La Niña episodes, cooler tropical Pacific conditions are associated with reduced atmospheric heating and greater ocean heat storage, so global mean temperatures tend to fall (McPhaden et al., 2020). The atmospheric counterpart of these oceanic anomalies is the Southern Oscillation, which captures changes in pressure, winds, and atmospheric circulation across the tropical Pacific.

Figure 1: Sea Surface Temperature Comparison

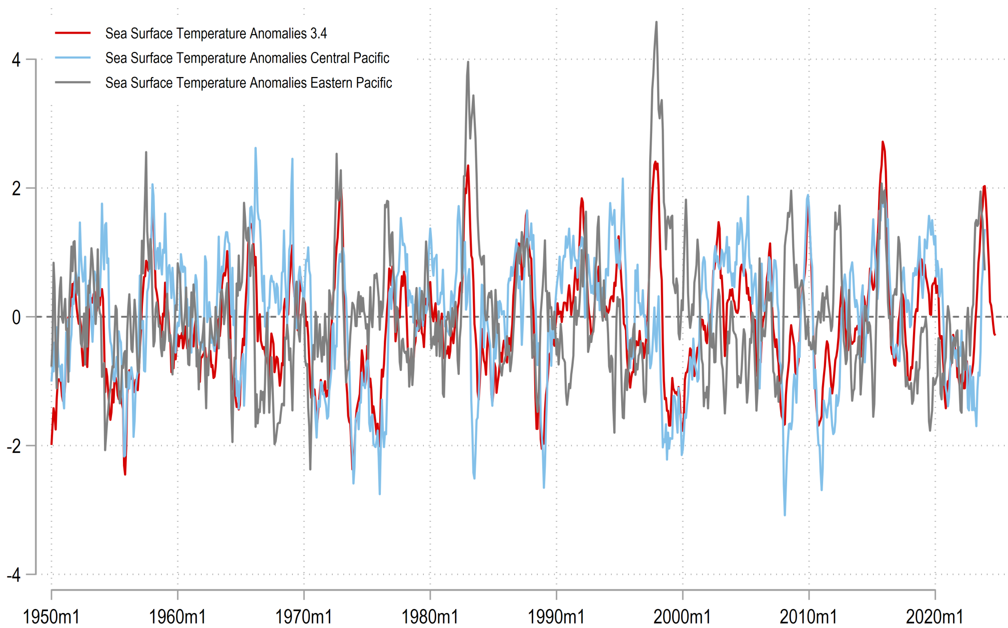

Figure 1 compares the baseline Niño 3.4 SST anomaly with the Central-Pacific (CP) and Eastern-Pacific (EP) ENSO anomaly measures. All three series fluctuate around zero, confirming the recurrent alternation between warm and cold ENSO conditions. However, the figure also shows that the three measures are not interchangeable. The Niño 3.4 index captures broad ENSO variability, while the CP and EP indices display distinct timing, amplitude, and persistence. Several major episodes, such as the early 1980s, late 1990s, and mid-2010s events, are visible in the Niño 3.4 series, but their intensity differs markedly across the CP and EP measures. In particular, EP anomalies exhibit large spikes during some canonical El Niño episodes, whereas CP anomalies display a different pattern of fluctuations across the sample. This visual evidence motivates the empirical distinction between baseline, CP, and EP ENSO shocks, since spatially different SST anomalies may generate different teleconnection patterns and therefore different oil-price responses.

2.2. Economic Data

The model includes world industrial output (Y_t);[1] U.S. WTI (West Texas Intermediate) oil futures prices (op_t^F) on the New York Mercantile Exchange (NYMEX), which is part of the Chicago Mercantile Exchange Group (CME); the U.S. WTI oil spot price (op_t^G); global oil (o_t) production (million barrels per day); and the U.S. nominal effective exchange rate $(NEER_t)$. The sample period is monthly and covers 1983:03 to 2024:10. We utilize SST anomalies in the Niño 3.4 region as the primary indicator of ENSO, collected from the National Oceanic and Atmospheric Administration (NOAA).

[1] Coming from an updated version of the dataset in Baumeister and Hamilton (2019).

The oil futures and spot prices are seasonally adjusted via ARIMA X-12 algorithm from the U.S. Census Bureau. The oil futures and spot prices, denominated in U.S. dollars, are deflated by the U.S. consumer price index (CPI). The data are summarized in Tables 1 and 2. We plot the economic data in Figure 2.

Table 1: Variable Selection

Item	Symbol	Source	Description
World Output	Y_t	See [a]	World Industrial Production
Aggregate CPI	P_t	OECD	U.S. CPI: All items
Oil Futures Price	$op_t^{WTI,F}$	CME	U.S. WTI Futures Price
Oil Spot Price	$op_t^{WTI,G}$	FRED	U.S. WTI Spot Price
Exchange Rate	$\ln NEER_t$	BIS	U.S. Nominal Effective Exchange Rate
Oil Production	o_t	EIA	Global Crude Oil Production
ENSO	SST_t	NOAA	Niño 3.4 SST anomaly
El Niño 3.4 SST Anomaly	s_t^{EN}	NOAA	Absolute SST anomaly in El Niño months
La Niña 3.4 SST Anomaly	s_t^{LN}	NOAA	Absolute SST anomaly in La Niña months
Central-Pacific ENSO	CP_t	See [b]	Central-Pacific ENSO anomaly
Eastern-Pacific ENSO	EP_t	See [b]	Eastern-Pacific ENSO anomaly

[a]: See https://sites.google.com/site/cjsbaumeister/datasets.
[b]: CP and EP ENSO measures follow Kao and Yu (2009) and Yu and Kim (2010).

Table 2: Summary Statistics

Item	Symbol	Obs.	Mean	Std. dev.	Min.	Max.
World Output	$\ln Y_t$	499	4.507	0.326	3.860	4.981
Oil Futures Price	$\ln op_t^{WTI,F}$	499	2.080	0.448	1.000	3.167
Oil Spot Price	$\ln op_t^{WTI,G}$	499	2.173	0.445	1.000	3.192
Exchange Rate	$\ln NEER_t$	500	4.605	0.128	4.357	5.014
Oil Production	$\ln o_t$	500	4.229	0.138	3.927	4.438
ENSO	SST_t	500	-0.058	0.892	-2.050	2.720
Eastern-Pacific ENSO	EP_t	490	0.060	1.067	-1.800	4.580
Central-Pacific ENSO	CP_t	490	-0.004	1.042	-3.083	2.147
El Niño 3.4 SST Anomaly	s_t^{EN}	500	0.329	0.550	0.000	2.720
La Niña 3.4 SST Anomaly	s_t^{LN}	500	0.386	0.488	0.000	2.050

Note: The table reports summary statistics for the main variables used in the local-projection specifications. The sample starts in 1983m3. Oil futures and spot prices are real WTI prices expressed in logs. World output, global crude-oil production, and the U.S. nominal effective exchange rate are also expressed in logs. SST_t denotes the Niño 3.4 sea-surface-temperature anomaly. EP_t and CP_t denote the Eastern-Pacific and Central-Pacific ENSO anomaly measures, respectively. s_t^{EN} and s_t^{LN} correspond to SSTEN and SSTLN: the absolute Niño 3.4 SST anomalies during El Niño and La Niña episodes, respectively, and zero otherwise. Their sample means, 0.33°C and 0.39°C, are used to scale the one-degree impulse responses reported in the text. The aggregate CPI reported in Table 1 is used to deflate nominal oil prices and is therefore not reported separately.

Figure 2 shows pronounced low-frequency variation in the macroeconomic and oil-market variables over the sample. World industrial output and the U.S. consumer price index trend upward, with temporary slowdowns or declines around shaded NBER recessions. Real WTI futures and spot prices display substantial co-movement, reflecting their common exposure to global oil-market fundamentals, while also exhibiting large cyclical movements around major macroeconomic and oil-market disruptions, including the early 1990s, the global financial crisis, and the COVID-19 episode. The nominal effective exchange rate follows independent U.S. dollar valuation cycles, which is important because oil prices are denominated in dollars. Global crude-oil production trends upward over the sample but displays interruptions around major downturns, most visibly during the pandemic.

The SST anomaly series fluctuates around zero and alternates between positive El Niño and negative La Niña phases. Large positive anomalies are visible during major El Niño episodes, including the late 1990s and the mid-2010s, while negative anomalies capture La Niña conditions. The coexistence of persistent macroeconomic variables and recurrent climate oscillations motivates the use of monthly controls and a rich lag structure in the local-projection specifications. It also supports the empirical distinction between ENSO variation and conventional oil-market fundamentals: the estimation conditions on global demand, oil supply, exchange-rate movements, and lagged dynamics while using phase-specific SST anomalies to trace the climate component of oil-price responses.

Figure 2: Economic Data

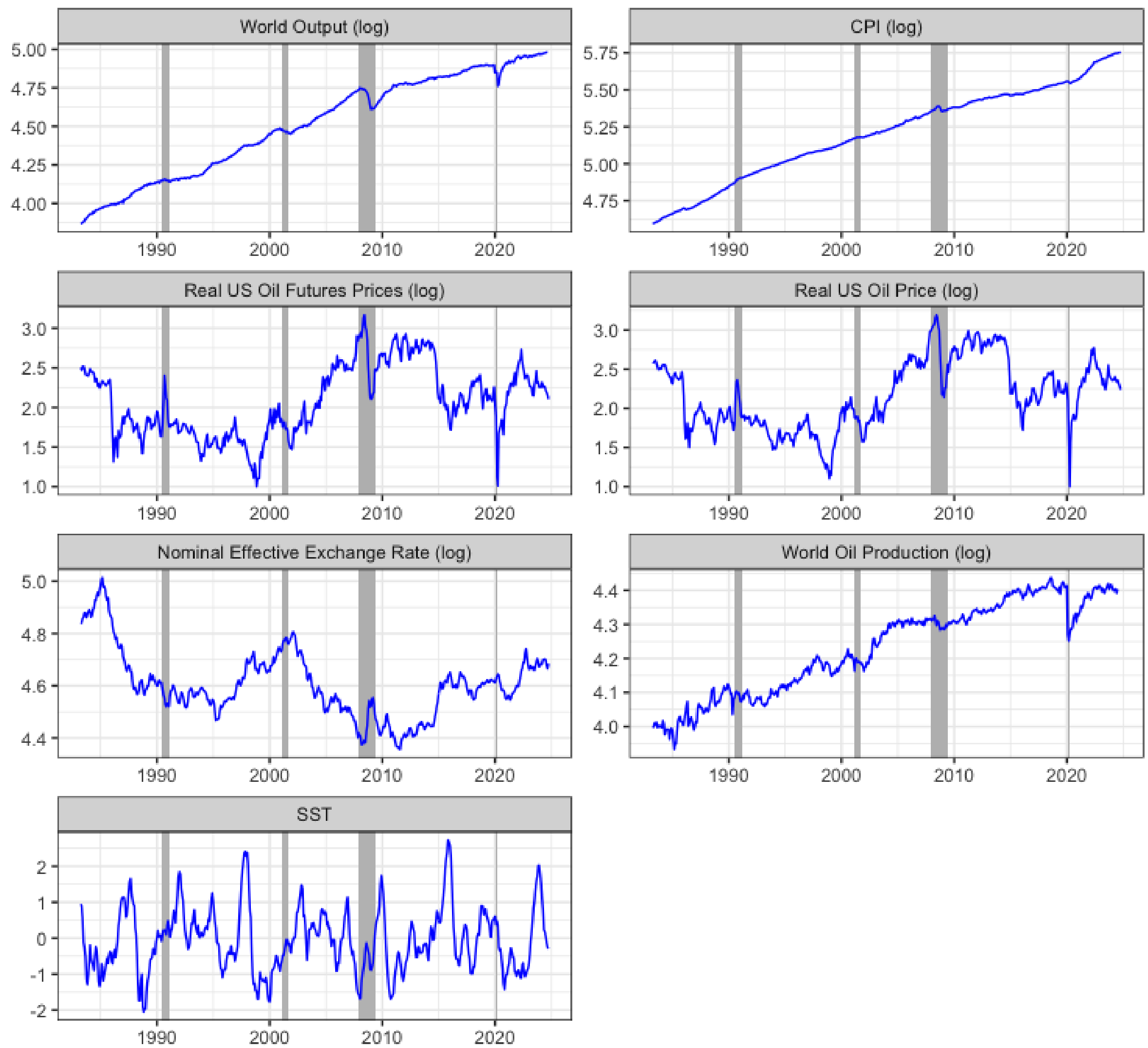

Note: Shaded areas indicate NBER recession dates.

The figure further shows that the oil-price series, macroeconomic fundamentals, and ENSO anomalies do not move mechanically with the same timing. Real WTI futures and spot prices exhibit sharp movements around major downturns, but also display large fluctuations outside NBER recession windows, consistent with oil-specific supply, demand, financial, and geopolitical forces. The futures and spot series are highly correlated, yet not identical, which is consistent with the role of futures prices in incorporating expectations before all information is reflected in the physical market. By contrast, the SST anomaly series follows a climate-driven oscillatory pattern that is visually distinct from the macroeconomic trends in output, prices, production, and the exchange rate. This separation reinforces the empirical role of ENSO anomalies as external climate variation, while the persistent macroeconomic series justify conditioning on fundamentals and lagged dynamics.

3. Methodology

Impulse responses are estimated using local projections (LPs) (Jordà, 2005) and then extended to the time-varying-parameter local projection (TVP-LP) estimator of Inoue et al. (2024). In a standard LP, the horizon-specific coefficient β_h summarizes the average response of oil prices at date $t + h$ to an ENSO anomaly observed at date t over the full sample. The TVP-LP generalizes this framework by allowing the response coefficient to vary with the calendar date of the anomaly. This distinction is relevant because ENSO transmission to oil futures and spot prices may depend on climate-risk salience, oil-market structure, global supply-chain conditions, and macroeconomic fundamentals.

The ENSO impulse variables are defined as phase-specific absolute SST anomalies. Specifically,

$$s_t^{EN} = |SST_t| \mathbf{1}\{EN_t = 1\}, \qquad s_t^{LN} = |SST_t| \mathbf{1}\{LN_t = 1\}, \tag{1}$$

where SST_t is the Niño 3.4 anomaly measured in degrees Celsius. The impulse variable is therefore expressed in degrees Celsius, and the estimated coefficients are dynamic multipliers for a one-degree increase in the corresponding phase-specific absolute SST anomaly. In the data, s_t^{EN} and s_t^{LN} correspond to the absolute Niño 3.4 SST anomaly during El Niño and La Niña episodes, respectively, and zero otherwise. Their sample means are 0.33°C and 0.39°C (Table 2), which are used below to scale the one-degree impulse responses to representative phase-specific anomaly magnitudes.

The baseline constant-parameter LP is specified, for each horizon h, as

$$op_{t+h}^{WTI,x} = \alpha_h + \beta_h^p s_t^p + \sum_{j=1}^{12} \mathbf{\Gamma}'_{j,h} \mathbf{z}_{t-j} + u_{h,t+h}, \quad p \in \{EN, LN\}, \quad h = 0, 1, \dots, H. \tag{2}$$

The coefficient β_h^p measures the average response of oil futures or spot prices at horizon h to a one-degree increase in the phase-specific absolute SST anomaly over the full sample. This specification provides the time-invariant benchmark against which the time-varying estimates are compared. By construction, however, Equation (2) pools all shock dates and therefore imposes that an ENSO anomaly occurring during the late 1990s has the same transmission coefficient as an ENSO anomaly occurring after 2015.

The TVP-LP preserves the LP logic of estimating a separate projection for each horizon while allowing the corresponding coefficient path to evolve over time. For each horizon h, the model is specified as

$$op_{t+h}^{WTI,x} = \alpha_{h,t} + \beta_{h,t}^p s_t^p + \sum_{j=1}^{12} \mathbf{\Gamma}'_{j,h,t} \mathbf{z}_{t-j} + v_{h,t+h}, \quad p \in \{EN, LN\}, \quad h = 0, 1, \dots, H, \tag{3}$$

where $op_t^{WTI,x}$ is the real U.S. WTI price for $x \in \{G, F\}$, corresponding respectively to spot and futures prices. The vector $\mathbf{z}_t = \{\ln Y_t, \ln o_t, \ln NEER_t\}$ contains world industrial output, world crude-oil production, and the U.S. nominal effective exchange rate. World industrial output captures global demand conditions; crude-oil production reflects supply-side fundamentals; and the nominal effective exchange rate helps isolate the ENSO response from currency-driven oil-price movements. The exchange-rate control is important because oil prices, exchange rates, and interest rates are jointly linked in international commodity markets (Kilian and Zhou, 2022). The error term is $v_{h,t+h}$, and $H = 24$ in the empirical application.

The coefficient $\beta^{p}_{h,t}$ is the central object of interest. It measures the response, at horizon h, of oil futures or spot prices at date $t+h$ to a one-degree phase-specific ENSO anomaly observed at date t. The two subscripts have distinct interpretations: h indexes the response horizon, whereas t indexes the calendar date at which the transmission coefficient is evaluated. Thus, the TVP-LP yields a horizon-specific coefficient path $\{\beta^{p}_{h,t}\}_{t=1}^{T-h}$ rather than a single full-sample average coefficient. The constant-parameter LP is obtained as the restricted case in which $\alpha_{h,t} = \alpha_h$, $\beta^{p}_{h,t} = \beta^{p}_{h}$, and $\mathbf{\Gamma}_{j,h,t} = \mathbf{\Gamma}_{j,h}$ for all t.

Identification relies on the external nature of ENSO variation. Sea-surface-temperature anomalies in the Niño 3.4 region are generated by ocean–atmosphere dynamics, implying that contemporaneous WTI prices do not plausibly feed back into ENSO realizations. The identifying assumption is that, conditional on lagged macroeconomic fundamentals and oil-market controls, the phase-specific ENSO anomaly is predetermined with respect to oil-price innovations. The inclusion of world industrial output, global crude-oil production, the U.S. nominal effective exchange rate, and twelve monthly lags further absorbs slow-moving demand, supply, exchange-rate, and persistence channels that could otherwise confound the dynamic response. For example, at horizon $h = 6$, $\beta^{EN}_{6,1997:12}$ measures the estimated response of real WTI prices in 1998:06 to a one-degree El Niño anomaly occurring during the major late-1990s ENSO episode, conditional on the same information set and lag structure. By contrast, $\beta^{EN}_{6,2016:01}$ measures the estimated response of real WTI prices in 2016:07 to a one-degree El Niño anomaly occurring after 2015. Since the anomaly definition, controls, and lag length are held fixed, differences between these coefficients capture changes in oil-market transmission rather than changes in the underlying climate-shock measurement.

The TVP-LP estimator is a parameter-path estimator rather than a rolling-window or kernel-smoothed regression. Time variation is not generated by repeatedly estimating the model over overlapping subsamples, nor by assigning larger weights to observations close to a target date. For each horizon, the estimator treats the coefficient as a full-sample path and recovers that path under admissible degrees of parameter instability. The constant-parameter LP provides the benchmark, and the path estimator uses observation-by-observation score and Hessian information to construct candidate coefficient paths under alternative degrees of instability. These paths are combined according to the weighted-average-risk criterion. Repeating this procedure for all horizons produces a time-varying impulse-response surface over both horizons and calendar time.

The specification includes twelve monthly lags, corresponding to one full year of lagged information. This rich lag structure is designed to absorb short-run autocorrelation, delayed adjustment in oil markets, and lagged macroeconomic dynamics. Following Montiel Olea and Plagborg-Møller (2021), lag-augmented LP inference is valid under persistence and remains robust to moderate misspecification when the regression contains a sufficiently informative lag structure. Twelve monthly lags therefore provide a conservative approximation to the relevant monthly dynamics and support valid inference under persistent dynamics without requiring exact knowledge of the true lag order.

Inference is conducted on the recovered coefficient path itself. Pointwise confidence bands are computed for $\beta^{p}_{h,t}$ at each date and horizon. A response is statistically different from zero at a given date–horizon pair when the corresponding confidence band excludes zero. These bands are interpreted as pointwise tests of the time-varying response, not as formal pairwise equality tests across selected historical episodes. Robust standard errors are used for the baseline LP exercises; the qualitative results are robust to the use of Newey-West standard errors. This is also consistent with the best-practice discussion in Jordà and Taylor (2025), who explain that Newey–West HAC corrections are the conventional response to the moving-average structure of LP residuals and show that lag-augmented confidence bands perform very similarly to Newey–West bands under stationary data, while becoming somewhat more conservative when persistence is high. We therefore interpret the rich lag-augmented specification and the Newey–West correction as complementary approaches to the same inference problem rather than competing empirical designs.

4. Empirical Results

4.1. Time-Series Local Projections

Figure 3 plots the time-invariant LP impulse response functions (IRFs). Accordingly, the IRFs show that an El Niño (a La Niña) anomaly corresponds with lower (higher) oil futures and spot prices. This finding for futures prices also aligns with Dufrénot et al. (2026), such that La Niña tends to be more inflationary for the Brent oil price than El Niño.

Figure 3: Response of Oil Price to ENSO

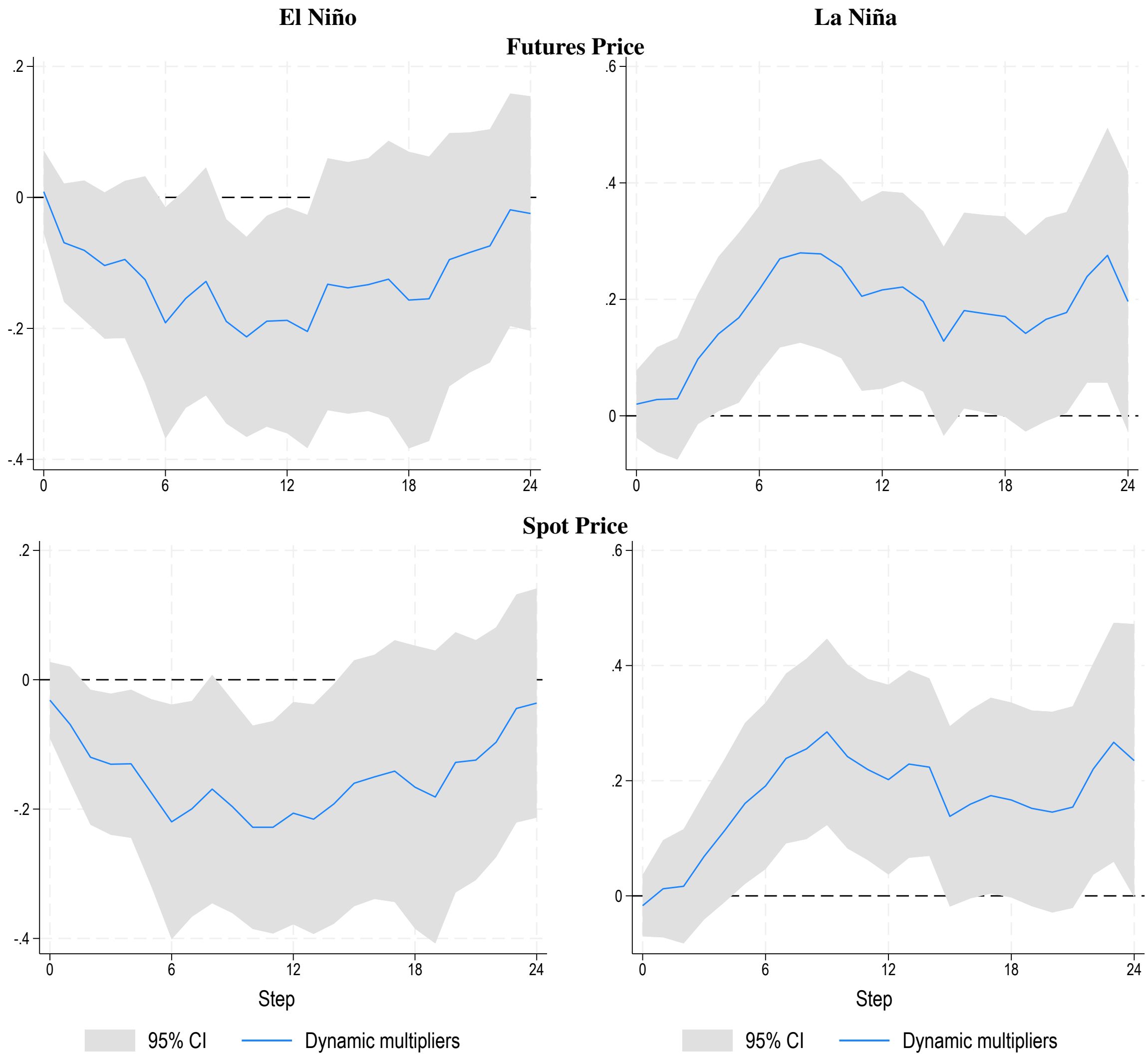

Figure 3 reports dynamic multipliers for a one-unit change in the phase-specific absolute SST anomaly. Since the dependent variables are log real oil prices, the coefficients are log-point responses. The approximate percentage response is $100\hat{\beta}$, while the exact percentage response is $100[\exp(\hat{\beta}) - 1]$. For the futures-price response, the El Niño coefficients at horizons 6–12 are −0.191, −0.154, −0.128, −0.189, −0.213, −0.189, and −0.188, respectively. These log-point responses correspond exactly to price changes of −17.4%, −14.3%, −12.0%, −17.2%, −19.2%, −17.2%, and −17.1%. The corresponding La Niña coefficients are 0.217, 0.270, 0.280, 0.278, 0.255, 0.205, and 0.216, which correspond exactly to price changes of 24.2%, 30.9%, 32.3%, 32.1%, 29.1%, 22.8%, and 24.1%. Thus, over the six- to twelve-month window, a one-degree El Niño anomaly is associated with a 12.0–19.2 percent decline in real WTI futures prices, while a one-degree La Niña anomaly is associated with a 22.8–32.3 percent increase. Scaling by the sample means of the phase-specific absolute impulse variables, 0.33°C for El Niño and 0.39°C for La Niña, yields implied declines of about 4.1% to 6.8% and increases of about 8.3% to 11.5%, respectively.

Figure 4: Oil Price Reaction to El Niño Across Time

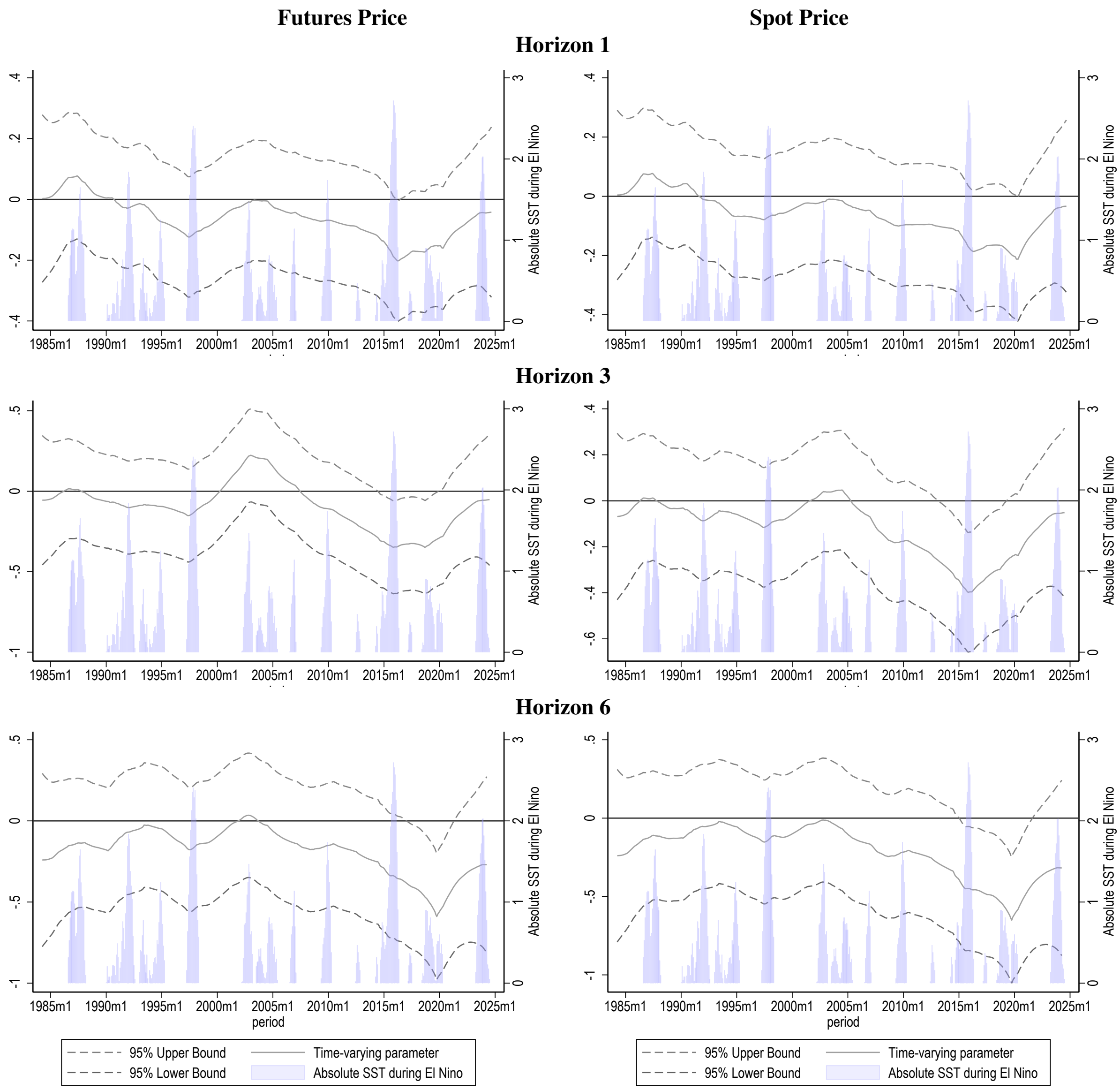

Note: Left (right) axis refers to IRFs (absolute SST during El Niño).

These magnitudes are large relative to much of the existing ENSO–commodity literature. For example, Brunner (2002) reports that a one-standard-deviation El Niño shock raises a broad index of non-oil primary commodity prices by about 3.5–4 percentage points. By contrast, our scaled futures-price responses imply declines of 4.1–6.8 percent for the mean El Niño impulse and increases of 8.3–11.5 percent for the mean La Niña impulse over the six- to twelve-month window. The comparison should be interpreted with caution because the objects differ: our dependent variable is the real WTI futures price rather than a broad non-oil commodity index, the impulse variables are phase-specific absolute Niño 3.4 anomalies measured in degrees

Celsius, and the effects are estimated at monthly medium horizons. Nevertheless, the contrast suggests that oil markets, and especially oil futures markets, are more sensitive to ENSO information than broad commodity aggregates.

Figure 5: Oil Price Reaction to El Niño Across Time (continued)

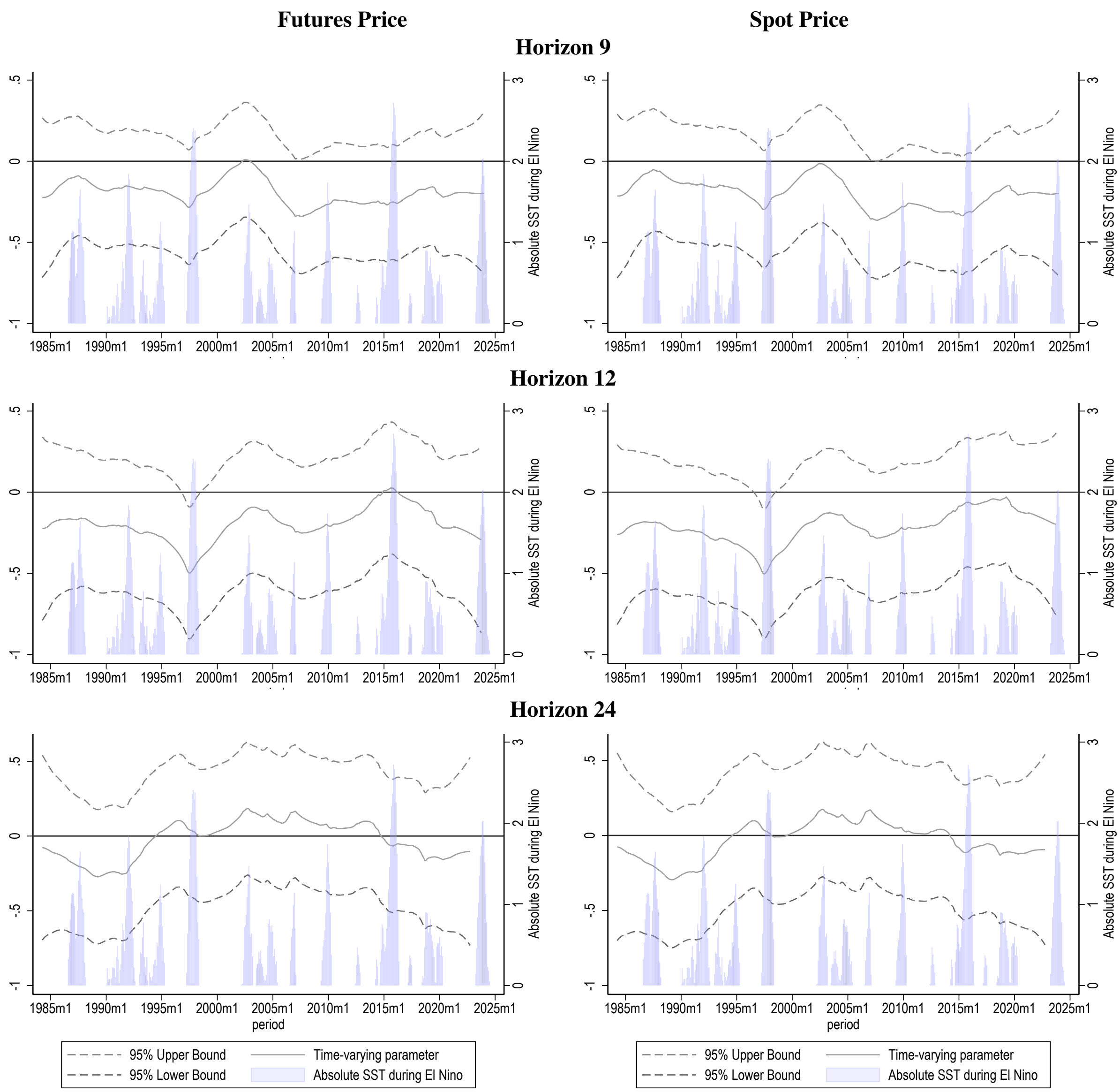

Note: Left (right) axis refers to IRFs (absolute SST during El Niño).

The larger magnitudes are also consistent with the mixed evidence in the oil-price literature. Cashin et al. (2017) find positive short-run oil-price effects of El Niño through higher demand from major industrial economies, whereas Solomou and Tian (2025) report negative effects. Changnon (1999) emphasizes that El Niño can reduce heating-oil demand, while Dufrénot et al. (2026) documents asymmetric effects across ENSO regimes and energy commodities. Our results help reconcile these findings by showing that the sign and magnitude of the oil-price response depend on ENSO phase, horizon, calendar time, and spatial ENSO type. Pooling El Niño and La Niña episodes, or imposing a time-invariant response, can attenuate the estimated effect. Once the shock is decomposed by phase and the coefficient is allowed to vary over time, La Niña emerges as the more inflationary oil-market shock, while El Niño is deflationary at medium horizons. The relatively large magnitudes therefore support the view that ENSO effects are amplified in oil markets through futures-market expectations, inventories, and delayed supply-demand adjustment.

4.2. Time-varying Climate-Risk Transmission

Figures 4–5 present the time-varying El Niño responses, Figures 6–7 present the time-varying La Niña responses, and Figures 8–9 summarize the baseline TVP-LP responses for futures and spot prices, including high-intensity ENSO events. These figures are central to the paper because they show that ENSO transmission is not stable across the sample. The estimated response depends jointly on the response horizon and on the calendar date of the climate anomaly.

Figure 6: Oil Price Reaction to La Niña Across Time

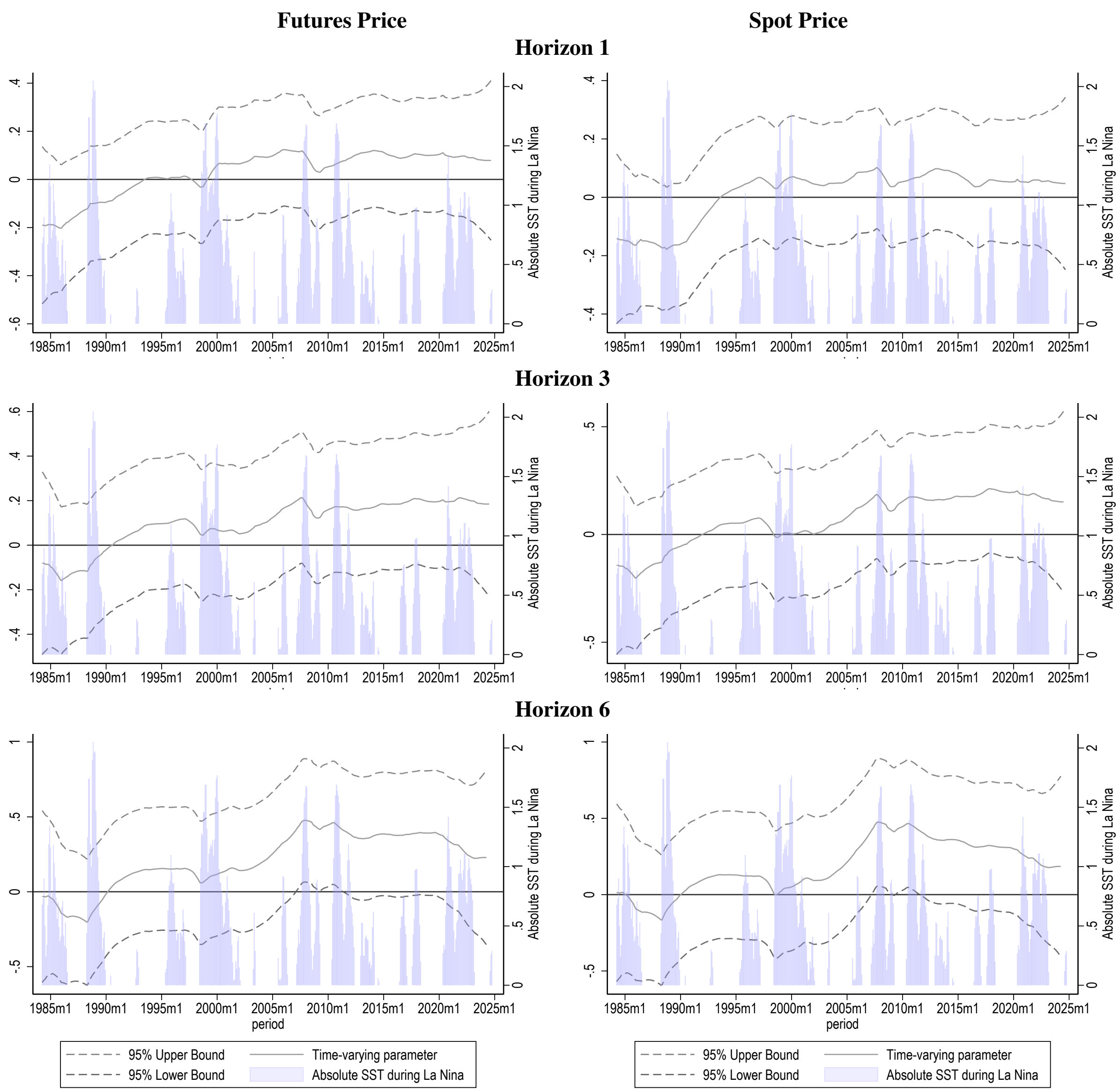

Note: Left (right) axis refers to IRFs (absolute SST during La Niña).

Figures 4 and 5 plot the TVP-LP responses of oil futures (left panel) and spot prices (right panel) to El Niño anomalies at horizons of 1, 3, 6, 9, 12, and 24 months. The solid line reports the time-varying coefficient, the dashed lines report the pointwise 95% confidence interval, and the shaded bars report absolute SST anomalies during El Niño episodes. The right-hand axis therefore indicates the physical intensity of El Niño conditions, while the left-hand axis reports the estimated oil-price response.

Figure 7: Oil Price Reaction to La Niña Across Time (continued)

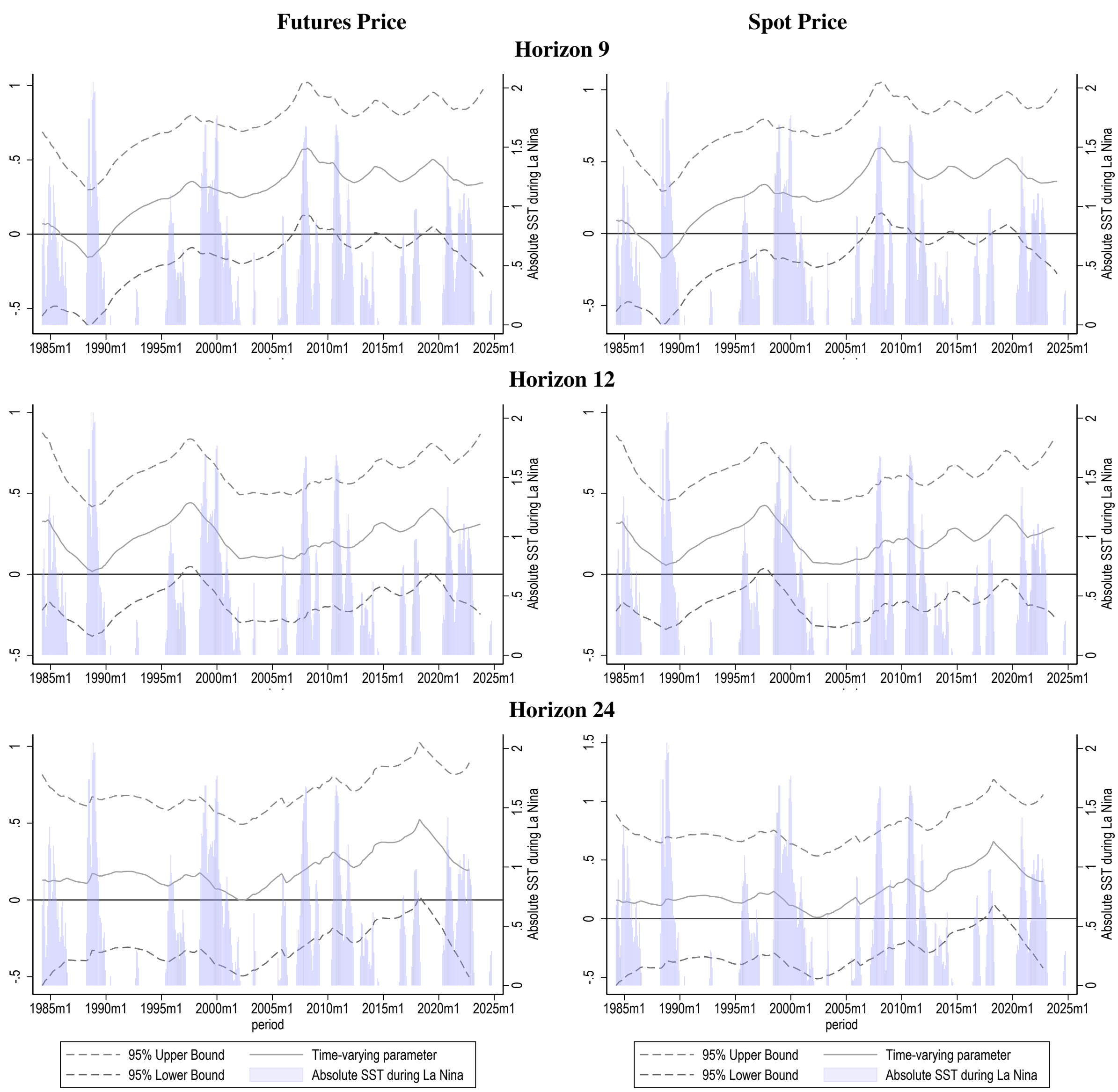

Note: Left (right) axis refers to IRFs (absolute SST during La Niña).

The El Niño response provides direct evidence of changing climate-risk transmission. Before the mid-1990s, the estimated response of futures and spot prices fluctuates around zero. In the more recent part of the sample, the response becomes more negative, especially at medium horizons.[2] At horizons 1, 3, and

[2] Borrallo et al. (2024) show that the ENSO newspaper popularity index spiked numerous times since 1996; prior to that period

6, the response becomes more negative from the mid-1990s onward and breaches the confidence bounds around the 2015 episode. By horizon 12, the response is persistently negative. This pattern suggests that recent El Niño episodes are not simply larger physical anomalies; rather, they are transmitted through a different market environment in which climate information, futures-market expectations, and anticipated energy-demand effects are priced more strongly. The delayed profile is consistent with adjustment through inventories, consumption, transportation, and broader macroeconomic conditions rather than an immediate contemporaneous response.

Figures 6 and 7 report the corresponding La Niña responses. The shaded bars capture absolute SST anomalies during La Niña episodes, while the solid line traces the time-varying oil-price response at each horizon.

Figure 8: Oil Futures Price Reaction to ENSO (TVP-LP)

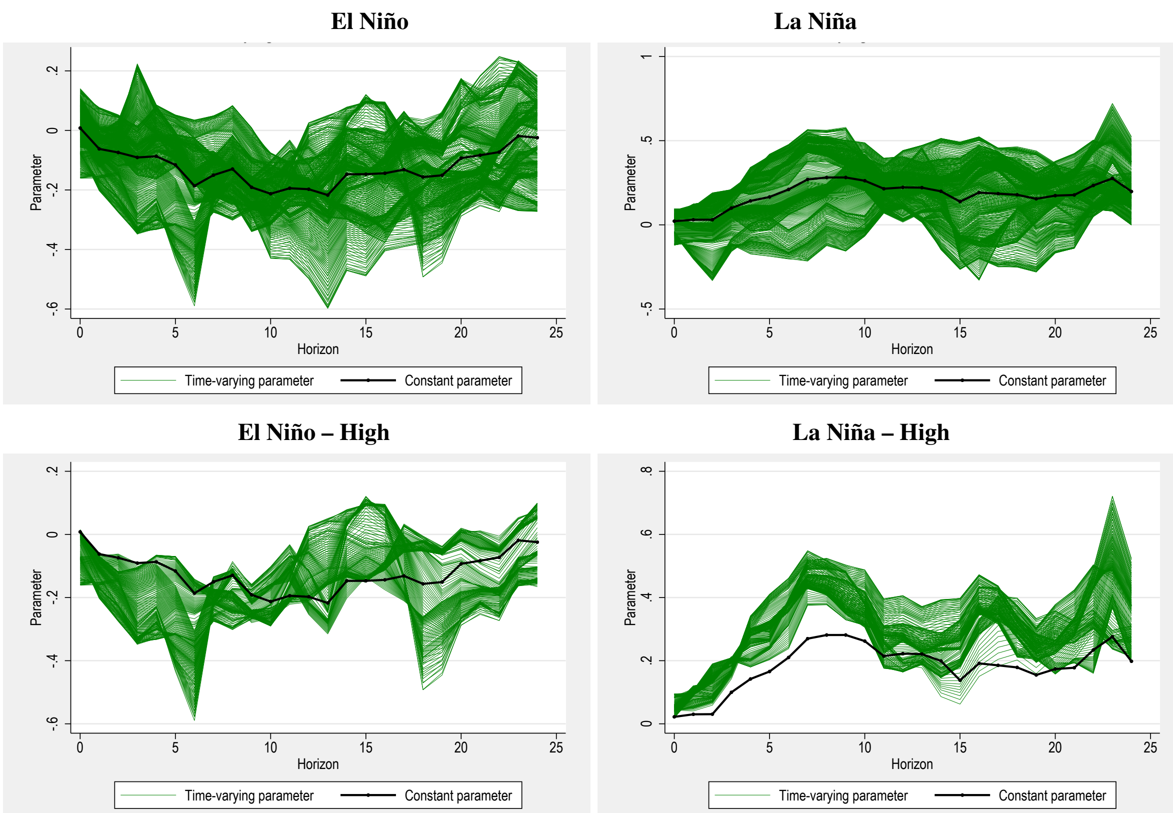

Note: "High" refers to anomalous El Niño (bottom left-panel) and La Niña (bottom right-panel) events defined as the top quartile (highest 25%) of the historical phase-specific anomaly distribution.

The La Niña results reinforce the asymmetric nature of ENSO transmission. Oil spot and futures prices tend to respond positively to La Niña anomalies, and the positive response becomes more visible in the recent part of the sample. The effect is especially apparent at medium horizons, including horizons 6, 9, and 12, which is consistent with delayed transmission through weather-sensitive demand, inventory pressures, transportation bottlenecks, production disruptions, and expectations of future market tightness. In contrast to El Niño, which is generally deflationary for oil prices, La Niña appears to operate as an inflationary climate-risk factor in oil markets. The recent strengthening of this response suggests that La Niña episodes

there were no spikes despite the 1982–83 El Niño being one of the strongest El Niño events recorded. NOAA began formally reporting on ENSO in the 1980s with the establishment of the Climate Prediction Center (CPC).

are priced in a market regime that is more sensitive to climate information and more exposed to delayed supply-demand pressures.

Figures 8 and 9 summarize the TVP-LP impulse-response surfaces for futures and spot prices. The top panels report the baseline El Niño and La Niña responses, while the bottom panels focus on high-intensity events defined as the top quartile (highest 25%) of the historical phase-specific anomaly distribution. The summary figures confirm the main message. El Niño responses are generally negative, La Niña responses are generally positive, and high-intensity events generate larger and more volatile responses. The stronger response to high-intensity La Niña events is particularly relevant for international macro-financial risk because it points to a climate-related source of oil-price pressure that can feed into inflation, energy prices, and policy trade-offs.

Figure 9: Oil Spot Price Reaction to ENSO (TVP-LP)

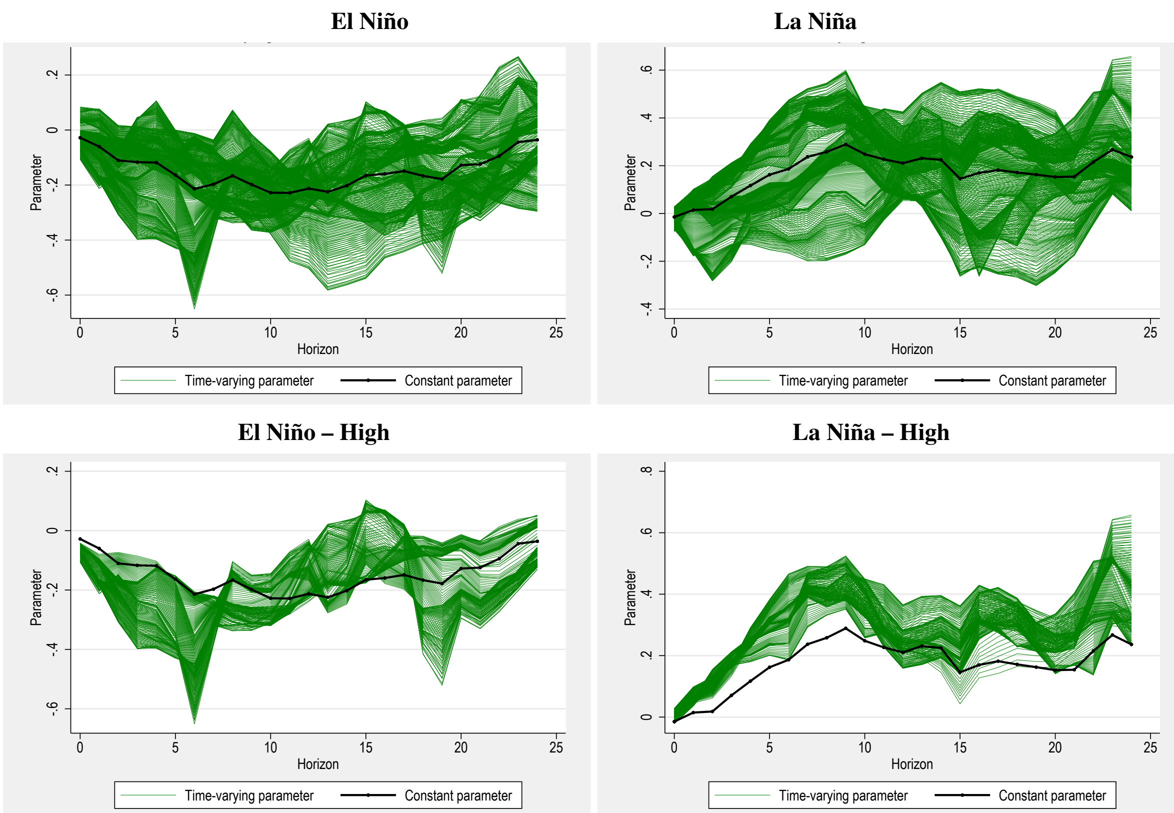

Note: "High" refers to anomalous El Niño (bottom left-panel) and La Niña (bottom right-panel) events defined as the top quartile (highest 25%) of the historical phase-specific anomaly distribution.

4.3. Climate-Risk Transmission Channels in International Oil Markets

Several channels can rationalize the time variation documented by the TVP-LP estimates. First, the climate-information channel may have strengthened over time. ENSO monitoring, forecasting, and public salience have improved substantially since the 1980s and especially since the late 1990s (Barnston, 2016; Borrallo et al., 2024). As information about ENSO conditions becomes more visible to traders, producers, policymakers, and financial-market participants, futures prices may incorporate expected climate-related demand and supply effects more rapidly. This mechanism is consistent with the stronger and more persistent time-varying responses observed in the recent part of the sample.

Second, futures-market expectations provide a direct link between ENSO and international oil pricing. Spot prices reflect realized physical-market conditions, while futures prices embed expectations about future demand, supply, inventories, financing conditions, and risk premia. This futures-market channel relates directly to evidence on time-varying risk premia in crude-oil futures (Hamilton and Wu, 2014). If market participants anticipate that El Niño will reduce heating-related energy demand or that La Niña will intensify demand and disruptions, these expectations can affect futures prices before the corresponding changes are fully visible in production, consumption, or inventories.

Third, ENSO affects oil prices through weather-sensitive energy demand. El Niño episodes are often associated with milder winter conditions in some major consuming regions, which can reduce heating demand and place downward pressure on oil prices (Changnon, 1999). La Niña episodes can generate the opposite pattern by intensifying cold-weather demand or increasing weather variability. Because these effects operate through inventories, expectations, and consumption adjustments, the response is naturally delayed and may be strongest at medium horizons.

Fourth, supply-side and logistical channels may amplify the response. ENSO phases affect rainfall, storm patterns, droughts, agricultural conditions, and transport networks across regions. These disturbances can alter refinery operations, shipping costs, inventory management, and broader supply-chain conditions (Cruz and Krausmann, 2013). La Niña episodes, in particular, may be associated with disruptions that raise expected marginal costs and generate upward pressure on energy prices.

Fifth, the strength of ENSO transmission depends on the structure of the oil market itself. Changes in OPEC behavior, the rise of U.S. shale production, financialization of commodity markets, inventory practices, speculative activity, cross-market linkages, and the growing role of futures markets can all affect how a given climate anomaly is priced (Büyükşahin and Robe, 2014). The TVP-LP results therefore capture not only the physical climate disturbance, but also the evolving market environment through which that disturbance is transmitted. Since oil is dollar-denominated, the exchange-rate environment is also relevant: the nominal effective exchange rate helps separate climate-related oil-price movements from dollar valuation cycles.

Finally, the spatial structure of ENSO provides an additional transmission channel. CP and EP events generate different teleconnection patterns and therefore different regional effects on temperature, rainfall, trade, and production (Ashok et al., 2017; Strnad et al., 2022; Alizadeh, 2024). This helps explain why the baseline Niño 3.4 results mask heterogeneous responses across CP and EP specifications and why CP La Niña events appear more inflationary for oil prices.

4.4. Spatial ENSO Heterogeneity and Oil-Price Responses

We next examine whether spatial ENSO diversity has oil-market pricing implications. This extension is important because a single Niño 3.4 measure can mask distinct climate teleconnections. We therefore distinguish between Eastern-Pacific (EP) and Central-Pacific (CP) ENSO types (McPhaden et al., 2020; Yu and Kao, 2007; Yu and Kim, 2010). These two regimes differ in their spatial structures, intensities, and temporal evolution (Geng et al., 2022; Dieppois et al., 2021; Capotondi et al., 2020). The distinction is economically meaningful: different teleconnections can affect regional temperature, rainfall, energy demand, production, transport, and inventories in different ways, and these differences may be priced differently in global oil markets.

To capture the spatial characteristics of EP and CP El Niño events, we employ the dataset developed by Kao and Yu (2009). CP events exhibit a stronger correlation with sea surface temperature (SST) anomalies (0.67), while EP events show a weaker association (0.38), underscoring their distinct spatial signatures. Our cross-correlation analysis further confirms that ENSO anomalies are heterogeneous rather than uniform. Although SST anomalies are commonly used as a proxy for ENSO activity, our findings reveal that EP and CP events follow distinct dynamic patterns.

These different ENSO types affect climate teleconnections. Several studies (Ashok et al., 2017; Strnad et al., 2022; Alizadeh, 2024) have shown that CP and EP events have very different climate teleconnections;

for example, while EP-ENSO is associated with heavy rain in Western South America, CP-ENSO shifts this impact away from Latin America.

The IRFs for the CP and EP ENSO shocks for spot and futures prices are reported in Figures A.1 and A.8, respectively. The results highlight important heterogeneity between CP and EP ENSO anomalies. For CP-type events (Figure A.1), El Niño shocks tend to exert a muted or slightly negative effect on both futures and spot prices, while La Niña shocks display more persistent upward pressure. By contrast, EP-type events (Figure A.8) exhibit a more pronounced and consistent negative response to El Niño shocks with effects that extend across multiple horizons. However, La Niña shocks in the EP regime show negative effects. Taken together, these patterns suggest that CP events are more inflationary for oil prices, especially during La Niña phases.

The impulse responses suggest that the mean effects of CP and EP ENSO shocks on oil prices are generally statistically insignificant, as indicated by the near-zero estimates from the constant-parameter specification. However, the distribution of time-varying estimates reveals that extreme El Niño and La Niña events, defined using the upper tail of the phase-specific anomaly distribution, tend to move oil prices away from the zero baseline. The TVP-LP impulse responses are plotted in Figures A.6–A.7 and Figures A.13–A.14 for CP and EP events, respectively. In particular, anomalous El Niño episodes are associated with negative deviations, while anomalous La Niña events generate positive swings, especially at medium horizons. These findings highlight that although the average response for CP and EP ENSO shocks is muted, extreme ENSO phases introduce considerable state-dependent volatility, underscoring a destabilizing role in the global oil market.

Figures A.2–A.5 report the horizon-specific CP El Niño and La Niña responses, while Figures A.9–A.12 report the corresponding EP responses. These figures complement the baseline results by showing that the timing and magnitude of oil-price responses vary not only across ENSO phases, but also across spatial ENSO types.

Overall, these results emphasize that distinguishing between EP and CP ENSO types is essential for correctly modeling climate-risk transmission to oil prices. At the same time, accounting for horizon-specific propagation and temporal variation through TVP IRFs reveals that the magnitude and persistence of these effects evolve across episodes, with CP La Niña and EP El Niño shocks emerging as the dominant inflationary and deflationary forces, respectively. Treating ENSO as a homogeneous and time-invariant phenomenon risks overlooking critical spatial differences in climatic drivers, their global teleconnections, and their dynamic macroeconomic consequences.

5. Conclusion

This paper studies how global climate shocks are transmitted to dollar-denominated oil spot and futures markets. Using phase-specific ENSO anomalies and a Time-Varying Parameter Local Projection framework, we show that ENSO-related oil-price risk is asymmetric, time-varying, and spatially heterogeneous. The results indicate that El Niño anomalies generally place downward pressure on real WTI spot and futures prices, while La Niña anomalies generate more persistent upward pressure. The effects are strongest at medium horizons, particularly within the six- to twelve-month window, which is consistent with delayed adjustment through expectations, inventories, weather-sensitive demand, supply disruptions, and global oil-market conditions.

The central contribution is the evidence of time-varying climate-risk transmission. A constant-parameter specification summarizes ENSO transmission through an average full-sample response, whereas the TVP-LP recovers the calendar-time path of the response at each horizon. The results show that the same measured SST anomaly can have different oil-price effects across historical periods. Recent ENSO episodes generate stronger responses than earlier episodes, suggesting that oil markets have become more responsive to climate information, futures-market expectations, supply-chain exposure, and evolving energy-market structure. This finding is important because it shifts the interpretation of ENSO from a fixed physical disturbance to a climate-risk factor whose market relevance changes over time.

The paper also documents spatial heterogeneity. Central-Pacific and Eastern-Pacific ENSO events transmit differently to oil prices, with CP La Niña episodes generating stronger inflationary pressure and EP El Niño episodes producing more muted or deflationary responses. This result shows that ENSO diversity is not merely a climatological refinement; it has economic content for oil-price dynamics and macro-financial risk assessment. Treating ENSO as a homogeneous and time-invariant shock risks overlooking important differences in the sign, timing, persistence, and magnitude of oil-price responses.

These findings have implications for international finance. Oil prices affect inflation, trade balances, energy costs, exchange rates, interest rates, and monetary-policy trade-offs. This interpretation is consistent with international finance evidence linking oil prices to exchange-rate and interest-rate dynamics (Kilian and Zhou, 2022; Ferraro et al., 2015). The results suggest that climate shocks are increasingly priced as global macro-financial risk factors in internationally traded commodity markets. Because the response depends on the ENSO phase, the response horizon, the calendar-time environment, and the spatial structure of the event, models that impose homogeneous and time-invariant climate effects may understate the risks associated with severe climate anomalies. Incorporating phase, temporal, and spatial heterogeneity is therefore essential for climate-informed forecasting, energy-market risk management, and the analysis of international risk transmission.

References

Ab Rahman, A. K., Abdullah, R., Balu, N. and Shariff, F. M. (2013), 'The impact of la niña and el niño events on crude palm oil prices: An econometric analysis', *Oil Palm Ind Econ J* **13**, 38–51.

Alexander, M., Bladé, I., Newman, M., Lanzante, J., Lau, N.-C. and Scott, J. (2002), 'The atmospheric bridge: The influence of ENSO teleconnections on air–sea interaction over the global oceans', *Journal of Climate* **15**(16), 2205–2231.

Alizadeh, O. (2024), 'A review of ENSO teleconnections at present and under future global warming', *Wiley Interdisciplinary Reviews: Climate Change* **15**(1), e861.

Ashok, K., Shamal, M., Sahai, A. and Swapna, P. (2017), 'Nonlinearities in the evolutional distinctions between El Niño and La Niña types', *Journal of Geophysical Research: Oceans* **122**(12), 9649–9662.

Atems, B. and Sardar, N. (2021), 'Exploring asymmetries in the effects of El Niño-Southern Oscillation on US food and agricultural stock prices', *The Quarterly Review of Economics and Finance* **81**, 1–14.

Balke, N., Plante, M. and Yücel, M. (2015), 'Fuel subsidies, the oil market and the world economy', *The Energy Journal* **36**, 99–128.

Barlow, M., Nigam, S. and Berbery, E. (2001), 'ENSO, pacific decadal variability, and US summertime precipitation, drought, and stream flow', *Journal of Climate* **14**(9), 2105–2128.

Barnston, A. G. (2016), 'Evolution of ENSO prediction over the past 40 years', *Climate Prediction S&T Digest* **94**.

Bastianin, A., Lanza, A. and Manera, M. (2018), 'Economic impacts of el niño southern oscillation: evidence from the colombian coffee market', *Agricultural Economics* **49**(5), 623–633.

Baumeister, C. and Hamilton, J. D. (2019), 'Structural interpretation of vector autoregressions with incomplete identification: Revisiting the role of oil supply and demand shocks', *American Economic Review* **109**(5), 1873–1910.

Bernanke, B., Gertler, M., Watson, M., Sims, C. and Friedman, B. (1997), 'Systematic monetary policy and the effects of oil price shocks', *Brookings Papers on Economic Activity* **1997**(1), 91–157.

Borrallo, F., Cuadro-Sáez, L., Ghirelli, C. and Pérez, J. J. (2024), '"El Niño" and "La Niña": Revisiting the impact on food commodity prices and euro area consumer prices', *Documentos de Trabajo/Banco de España, 2432* .

Brönnimann, S., Xoplaki, E., Casty, C., Pauling, A. and Luterbacher, J. (2007), 'ENSO influence on Europe during the last centuries', *Climate Dynamics* **28**(2-3), 181–197.

Brunner, A. D. (2002), 'El Nino and world primary commodity prices: warm water or hot air?', *Review of Economics and Statistics* **84**(1), 176–183.

Büyükşahin, B. and Robe, M. A. (2014), 'Speculators, commodities and cross-market linkages', *Journal of International Money and Finance* **42**, 38–70.

Capotondi, A., Wittenberg, A. T., Kug, J.-S., Takahashi, K. and McPhaden, M. J. (2020), 'ENSO diversity', *El Niño Southern Oscillation in a changing climate* pp. 65–86.

Cashin, P., Mohaddes, K. and Raissi, M. (2017), 'Fair weather or foul? The macroeconomic effects of El Niño', *Journal of International Economics* **106**, 37–54.

Changnon, S. A. (1999), 'Impacts of 1997–98 El Niño–generated weather in the United States', *Bulletin of the American Meteorological Society* **80**(9), 1819–1828.

Clements, B., Coady, D., Fabrizio, S., Gupta, S., Alleyne, T. and Sdralevich, C. (2013), *Energy subsidy reform: lessons and implications*, International Monetary Fund.

Coady, D., Parry, I., Sears, L. and Shang, B. (2017), 'How large are global fossil fuel subsidies?', *World Development* **91**, 11–27.

Cruz, A. M. and Krausmann, E. (2013), 'Vulnerability of the oil and gas sector to climate change and extreme weather events', *Climatic Change* **121**(1), 41–53.

Dai, A. (2013), 'Increasing drought under global warming in observations and models', *Nature Climate Change* **3**(1), 52–58.

Diaz, H. F., Hoerling, M. P. and Eischeid, J. K. (2001), 'ENSO variability, teleconnections and climate change', *International Journal of Climatology: A Journal of the Royal Meteorological Society* **21**(15), 1845–1862.

Dieppois, B., Capotondi, A., Pohl, B., Chun, K. P., Monerie, P.-A. and Eden, J. (2021), 'ENSO diversity shows robust decadal variations that must be captured for accurate future projections', *Communications Earth & Environment* **2**(1), 212.

Dufrénot, G., Ginn, W. and Pourroy, M. (2024), 'Climate pattern effects on global economic conditions', *Economic Modelling* p. 106920.

Dufrénot, G., Ginn, W. and Pourroy, M. (2026), 'Climate change impacts on commodity price stability through changing ENSO patterns', *World Development* **197**, 107165.

Ferraro, D., Rogoff, K. and Rossi, B. (2015), 'Can oil prices forecast exchange rates? an empirical analysis of the relationship between commodity prices and exchange rates', *Journal of International Money and Finance* **54**, 116–141.

Geng, T., Cai, W., Wu, L., Santoso, A., Wang, G., Jing, Z., Gan, B., Yang, Y., Li, S., Wang, S. et al. (2022), 'Emergence of changing central-pacific and eastern-pacific El Niño-Southern Oscillation in a warming climate', *Nature Communications* **13**(1), 6616.

Ginn, W. (2025), 'ENSO-augmented phillips curve: Evidence from panel local projections', *Oxford Bulletin of Economics and Statistics* .

Gutierrez, L. (2017), 'Impacts of El Niño-Southern Oscillation on the wheat market: A global dynamic analysis', *PloS one* **12**(6), e0179086.

Hamilton, J. D. and Wu, J. C. (2014), 'Risk premia in crude oil futures prices', *Journal of International Money and Finance* **42**, 9–37.

Iizumi, T., Luo, J.-J., Challinor, A. J., Sakurai, G., Yokozawa, M., Sakuma, H., Brown, M. E. and Yamagata, T. (2014), 'Impacts of El Niño Southern Oscillation on the global yields of major crops', *Nature Communications* **5**(1), 3712.

Inoue, A., Rossi, B. and Wang, Y. (2024), 'Local projections in unstable environments', *Journal of Econometrics* p. 105726.

Jordà, Ò. (2005), ‘Estimation and inference of impulse responses by local projections’, *American Economic Review* **95**(1), 161–182.

Jordà, Ò. and Taylor, A. M. (2025), ‘Local projections’, *Journal of Economic Literature* **63**(1), 59–110.

Kao, H.-Y. and Yu, J.-Y. (2009), ‘Contrasting eastern-pacific and central-Pacific types of ENSO’, *Journal of Climate* **22**(3), 615–632.

Kilian, L. and Zhou, X. (2022), ‘Oil prices, exchange rates and interest rates’, *Journal of International Money and Finance* **126**, 102679.

Laosuthi, T. and Selover, D. D. (2007), ‘Does El Niño affect business cycles?’, *Eastern Economic Journal* **33**(1), 21–42.

McPhaden, M. J., Santoso, A. and Cai, W. (2020), ‘Introduction to El Niño Southern Oscillation in a changing climate’, *El Niño Southern Oscillation in a Changing Climate* pp. 1–19.

McPhaden, M., Zebiak, S. and Glantz, M. (2006), ‘ENSO as an integrating concept in earth science’, *Science* **314**(5806), 1740–1745.

Montiel Olea, J. L. and Plagborg-Møller, M. (2021), ‘Local projection inference is simpler and more robust than you think’, *Econometrica* **89**(4), 1789–1823.

Qin, M., Su, C.-W., Hao, L.-N. and Tao, R. (2020), ‘The stability of us economic policy: Does it really matter for oil price?’, *Energy* **198**, 117315.

Ropelewski, C. F. and Halpert, M. S. (1987), ‘Global and regional scale precipitation patterns associated with the El Niño/Southern Oscillation’, *Monthly Weather Review* **115**(8), 1606–1626.

Rosenzweig, C., Iglesias, A., Yang, X., Epstein, P. and Chivian, E. (2001), ‘Climate change and extreme weather events’, *Global Change and Human Health* **2**(2), 90.

Solomou, S. and Tian, K. (2025), ‘The macroeconomic effects of El Niño diversity: a GVAR approach’, *Climate Research* . Forthcoming.

Strnad, F. M., Schlör, J., Fröhlich, C. and Goswami, B. (2022), ‘Teleconnection patterns of different El Niño types revealed by climate network curvature’, *Geophysical Research Letters* **49**(17), e2022GL098571.

Ubilava, D. (2012), ‘El Niño, La Niña, and world coffee price dynamics’, *Agricultural Economics* **43**(1), 17–26.

Ubilava, D. (2017), ‘The ENSO effect and asymmetries in wheat price dynamics’, *World Development* **96**, 490–502.

Yu, J.-Y. and Kao, H.-Y. (2007), ‘Decadal changes of ENSO persistence barrier in SST and ocean heat content indices: 1958–2001’, *Journal of Geophysical Research: Atmospheres* **112**(D13).

Yu, J.-Y. and Kim, S. T. (2010), ‘Identification of central-Pacific and eastern-Pacific types of ENSO in CMIP3 models’, *Geophysical Research Letters* **37**(15).

Appendix A. Appendix

Appendix A.1. Alternative Model: ENSO CP

Figure A.1 reports the constant-parameter LP responses for the Central-Pacific ENSO specification. It is placed at the start of the CP appendix because it provides the time-invariant benchmark before the horizon-specific TVP-LP figures.

Figure A.1: Response of Oil Price to CP ENSO

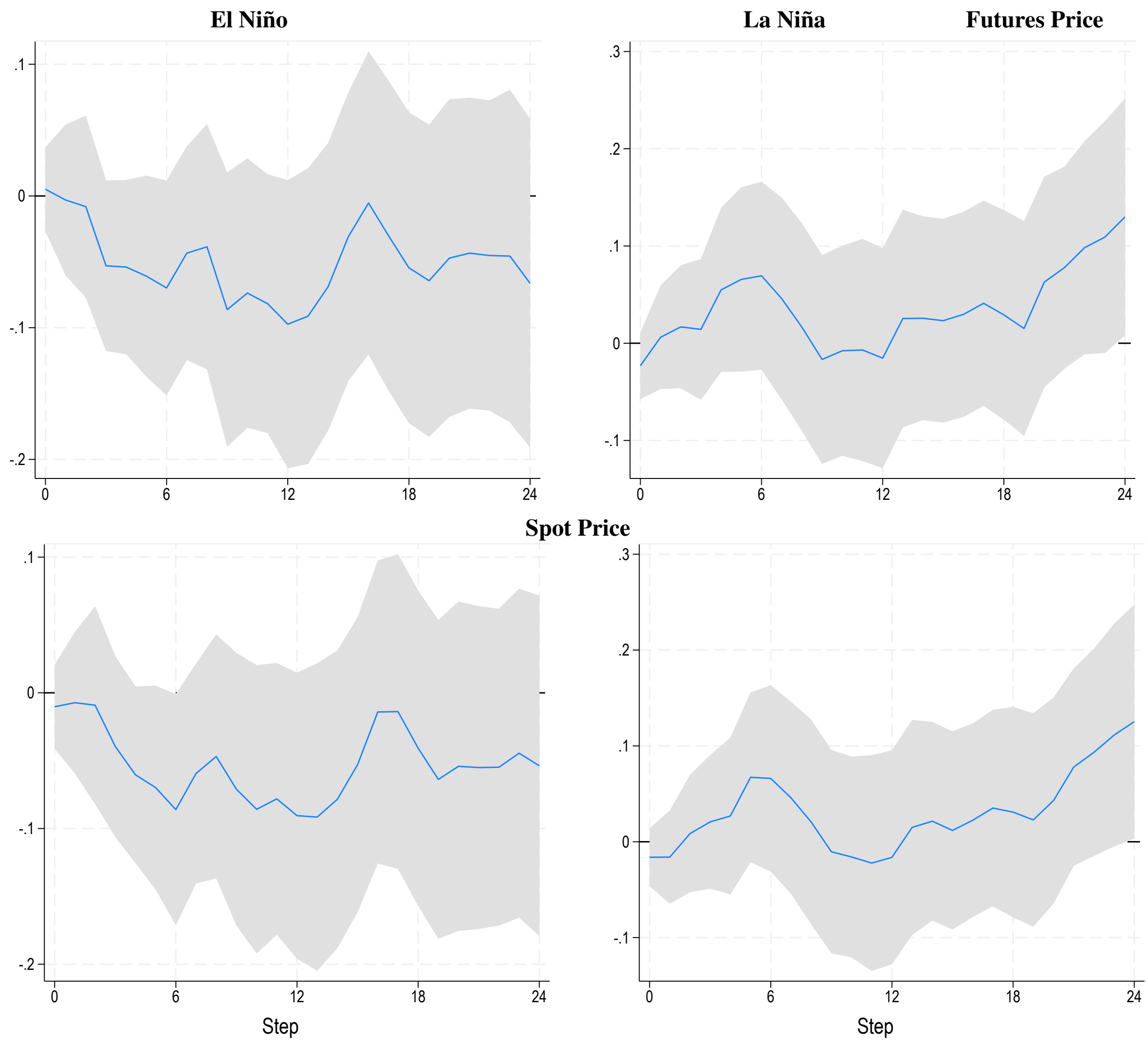

Figures A.2 and A.3 report the CP El Niño TVP-LP responses across the same horizons used in the baseline analysis.

Figure A.2: Oil Price Reaction to El Niño Across Time (CP ENSO)

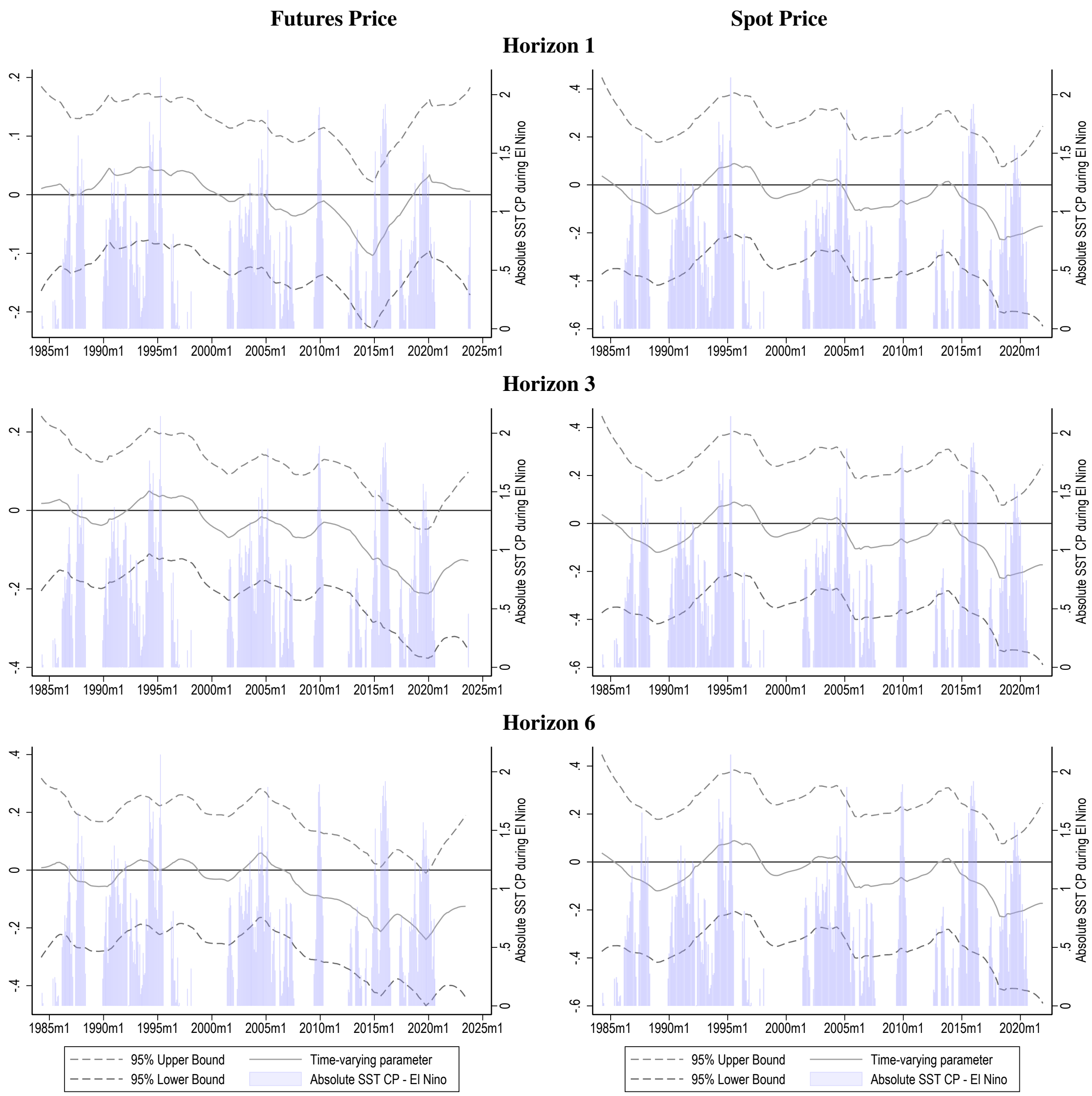

Note: Left (right) axis refers to IRFs (absolute SST during El Niño).

Figure A.3: Oil Price Reaction to El Niño Across Time (CP ENSO) (continued)

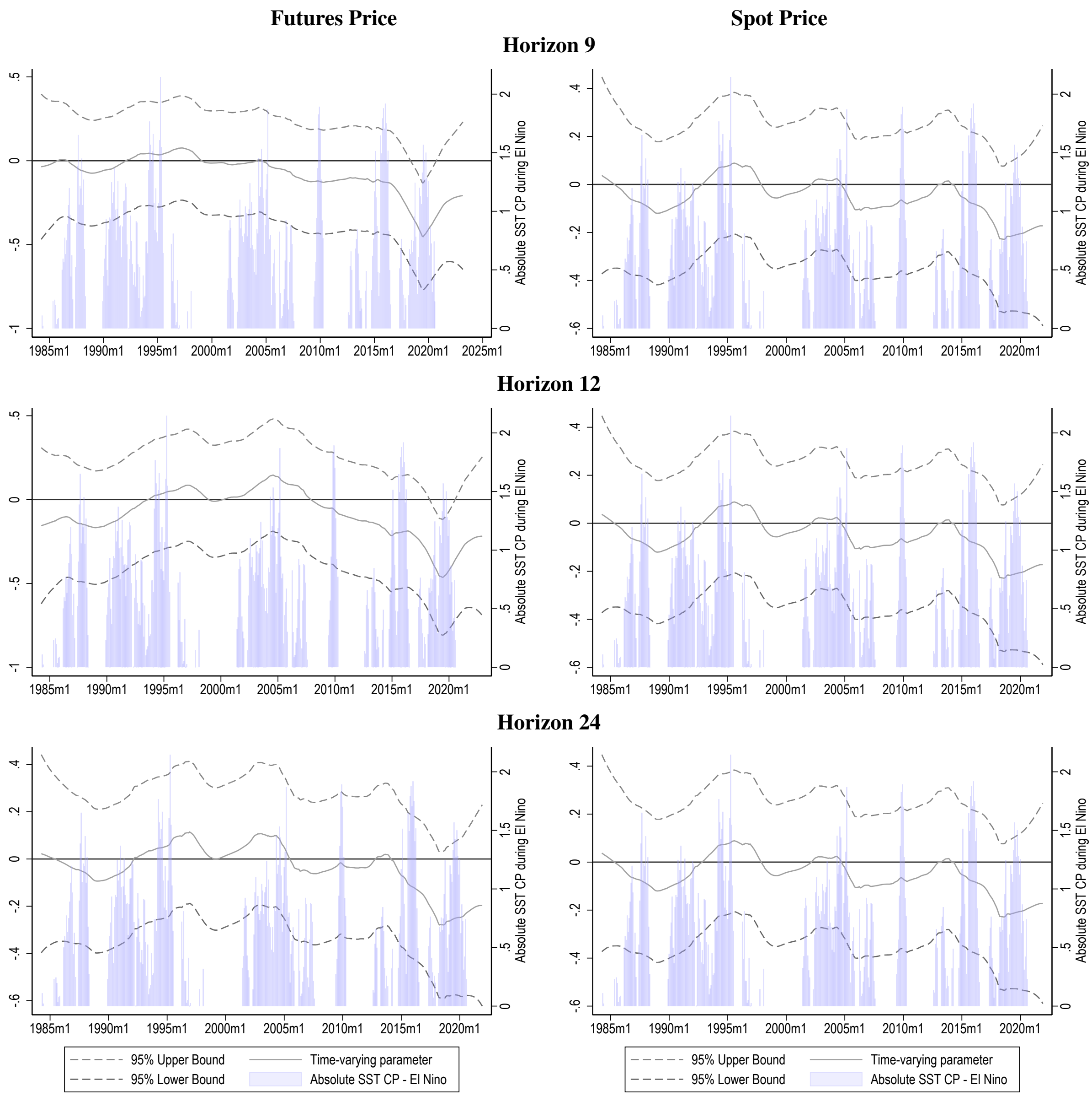

Note: Left (right) axis refers to IRFs (absolute SST during El Niño).

Figures A.4 and A.5 report the CP La Niña TVP-LP responses.

Figure A.4: Oil Price Reaction to La Niña Across Time (CP ENSO)

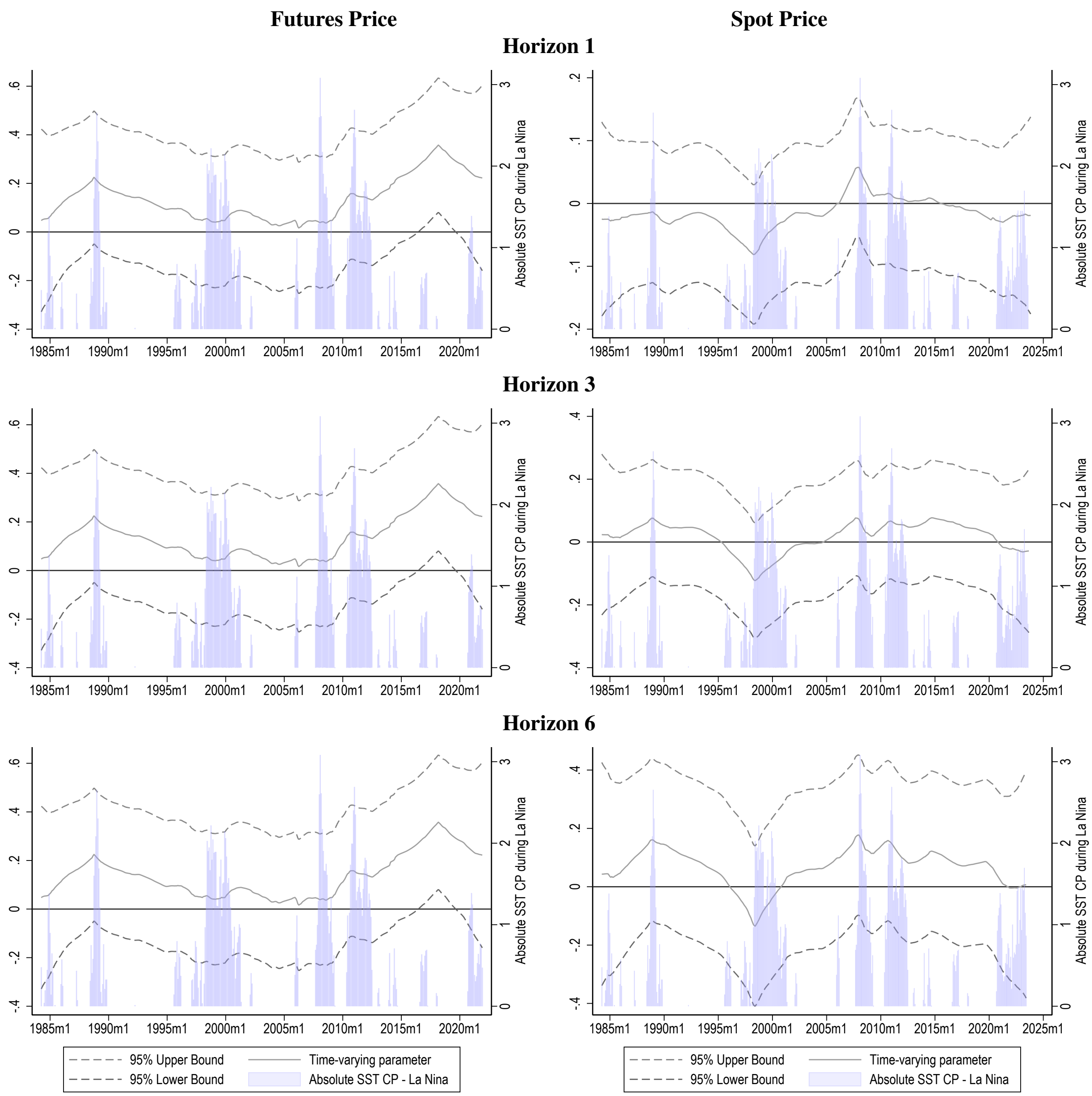

Note: Left (right) axis refers to IRFs (absolute SST during La Niña).

Figure A.5: Oil Price Reaction to La Niña Across Time (CP ENSO) (continued)

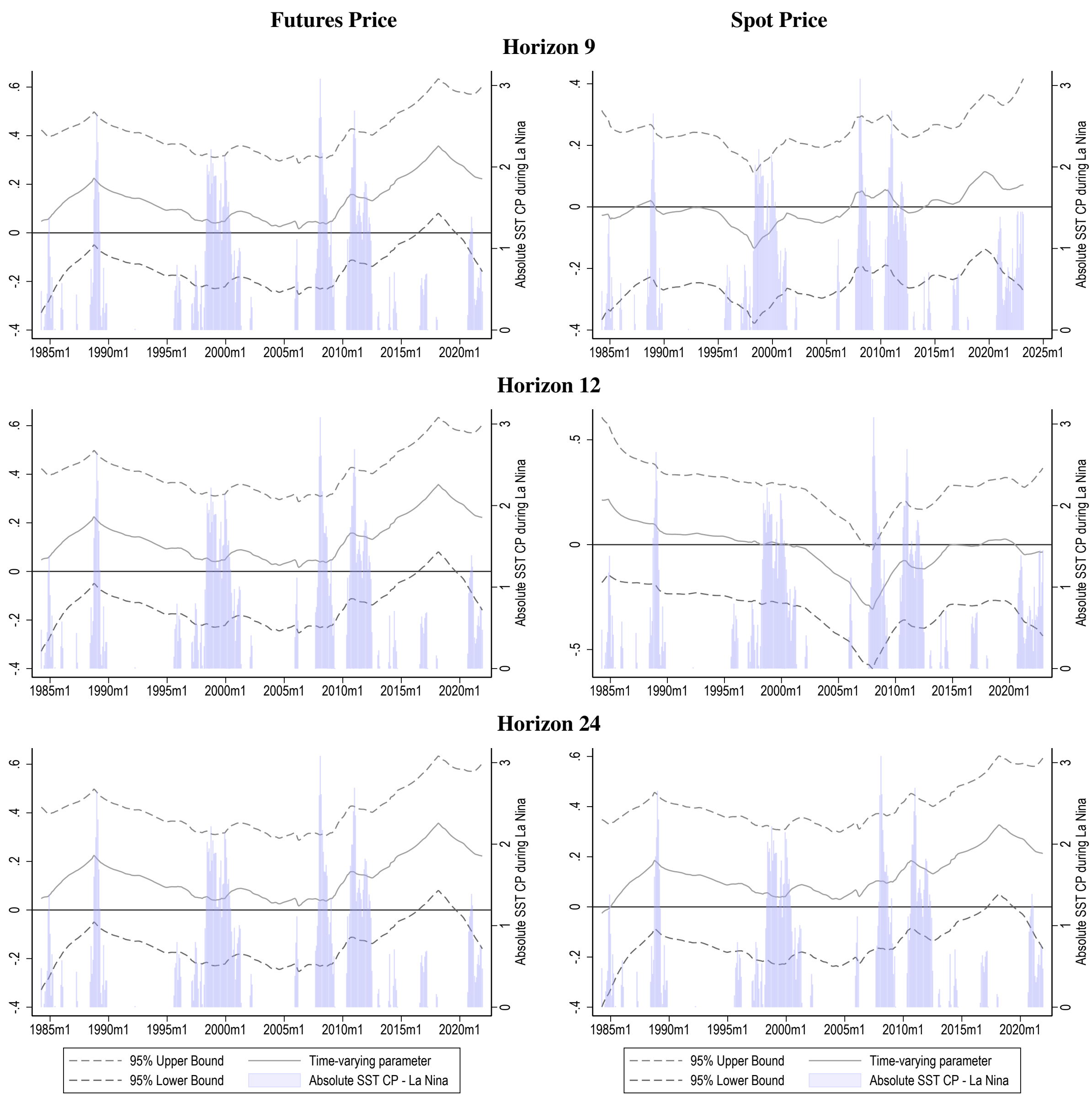

Note: Left (right) axis refers to IRFs (absolute SST during La Niña).

Figures A.6 and A.7 summarize the CP ENSO TVP-LP responses for futures and spot prices, including high-intensity ENSO events.

Figure A.6: Oil Futures Price Reaction to CP ENSO (TVP-LP)

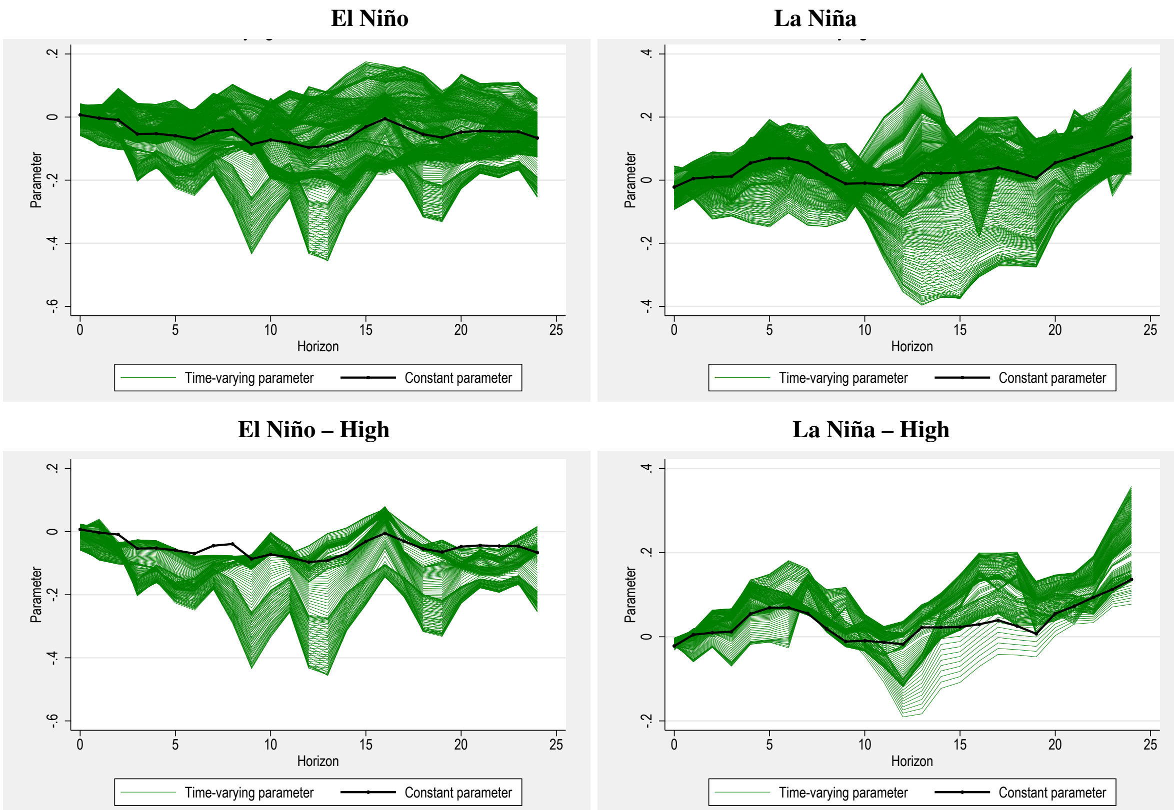

Note: "High" refers to anomalous El Niño and La Niña events defined as the top quartile (highest 25%) of the historical phase-specific anomaly distribution.

Figure A.7: Oil Spot Price Reaction to CP ENSO (TVP-LP)

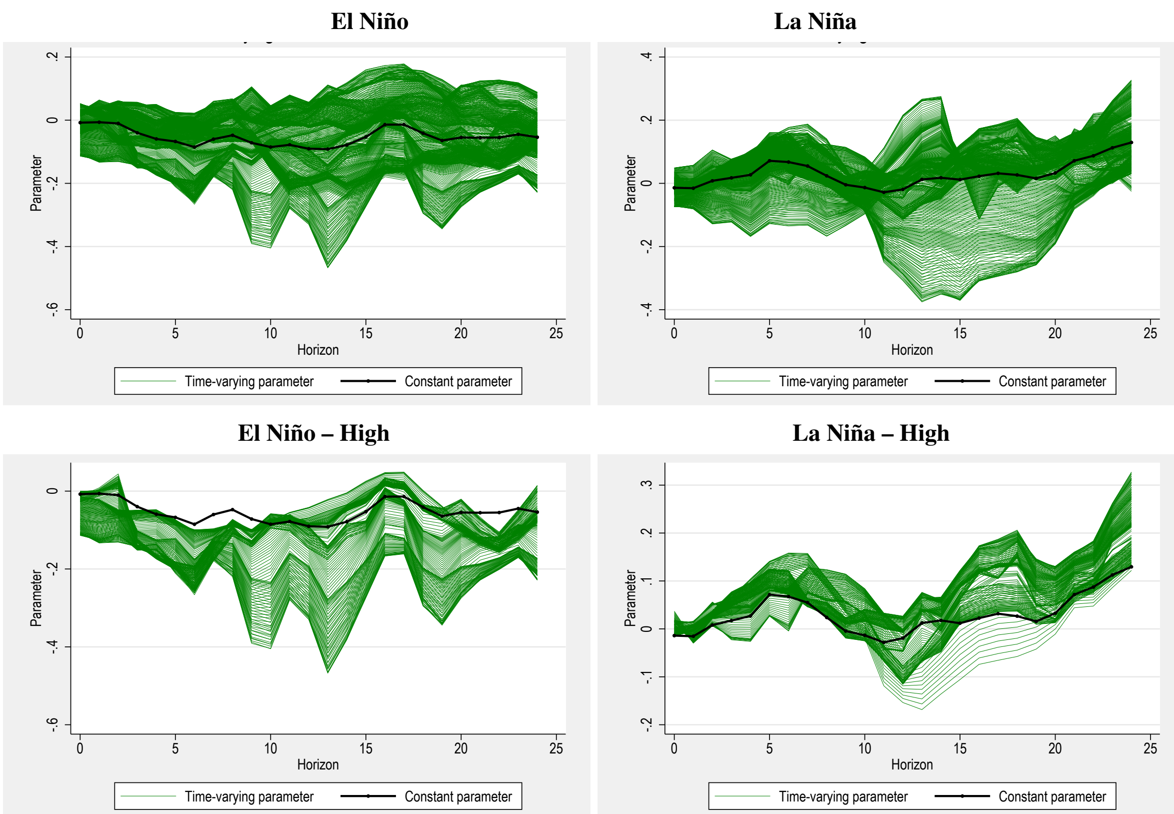

Note: "High" refers to anomalous El Niño and La Niña events defined as the top quartile (highest 25%) of the historical phase-specific anomaly distribution.

Appendix A.2. Alternative Model: ENSO EP

Figure A.8 reports the constant-parameter LP responses for the Eastern-Pacific ENSO specification. It mirrors the CP appendix structure and provides the time-invariant benchmark before the TVP-LP figures.

Figure A.8: Response of Oil Price to EP ENSO

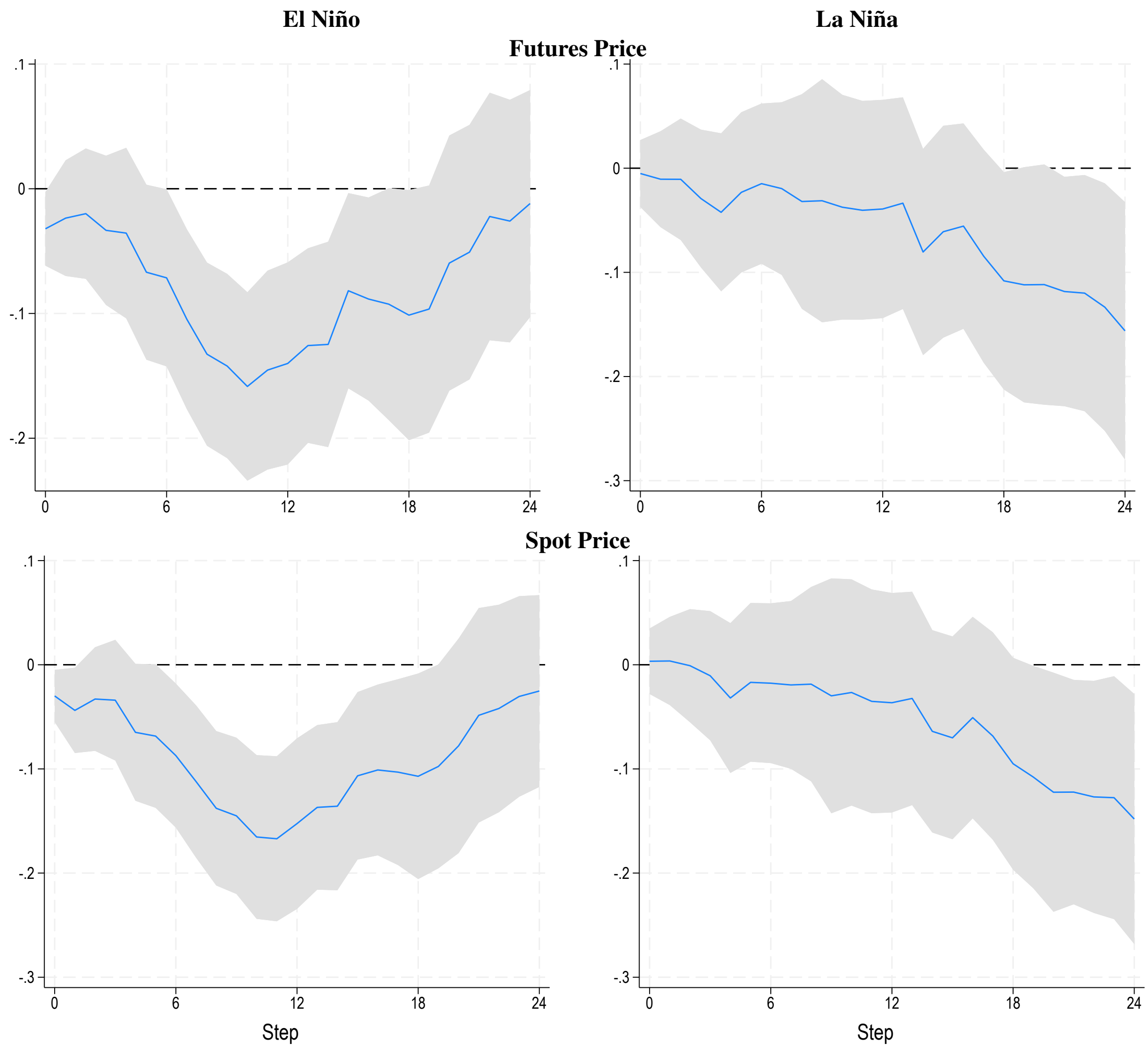

Figures A.9 and A.10 report the EP El Niño TVP-LP responses across horizons.

Figure A.9: Oil Price Reaction to El Niño Across Time (EP ENSO)

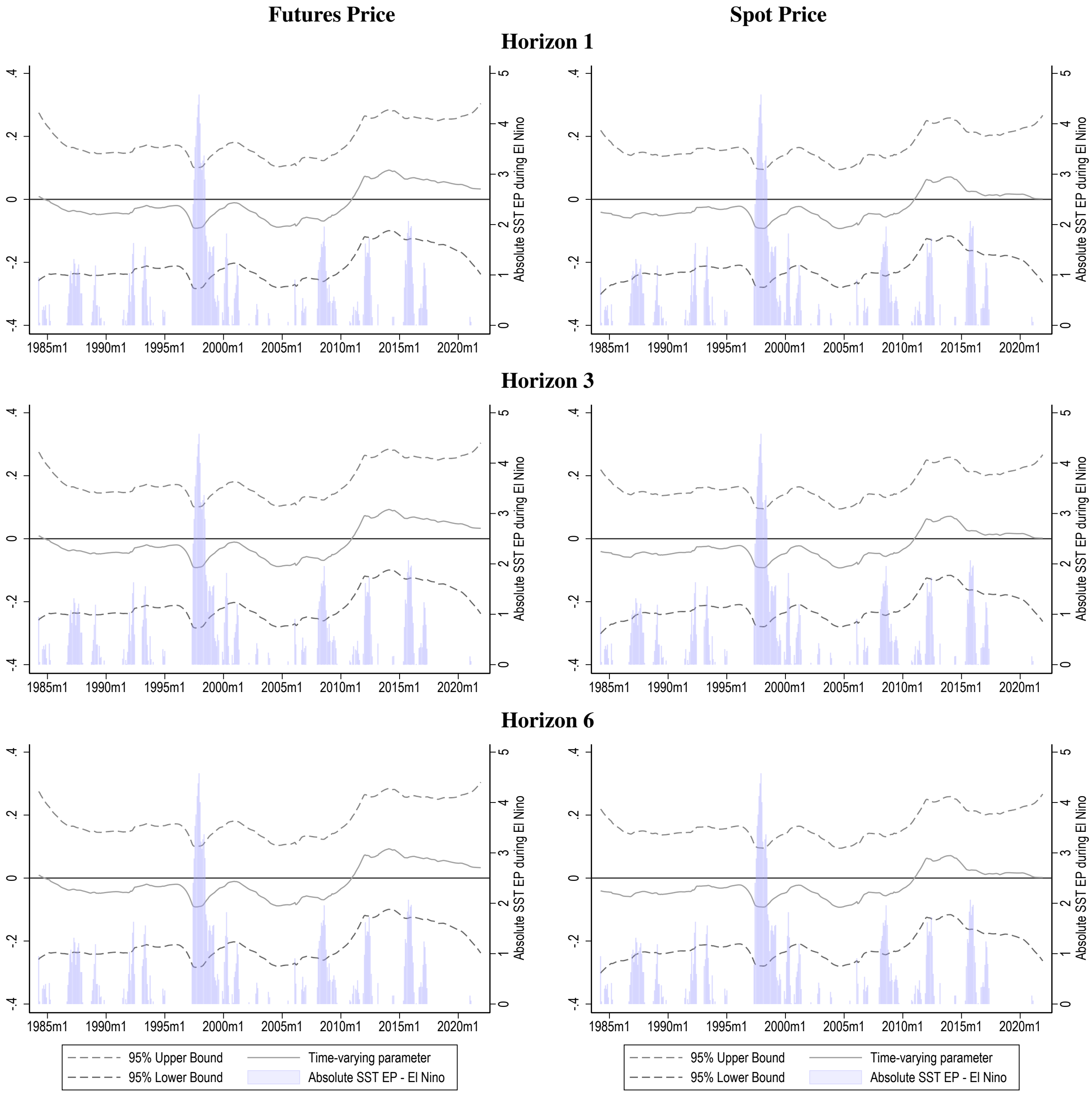

Note: Left (right) axis refers to IRFs (absolute SST during El Niño).

Figure A.10: Oil Price Reaction to El Niño Across Time (EP ENSO) (continued)

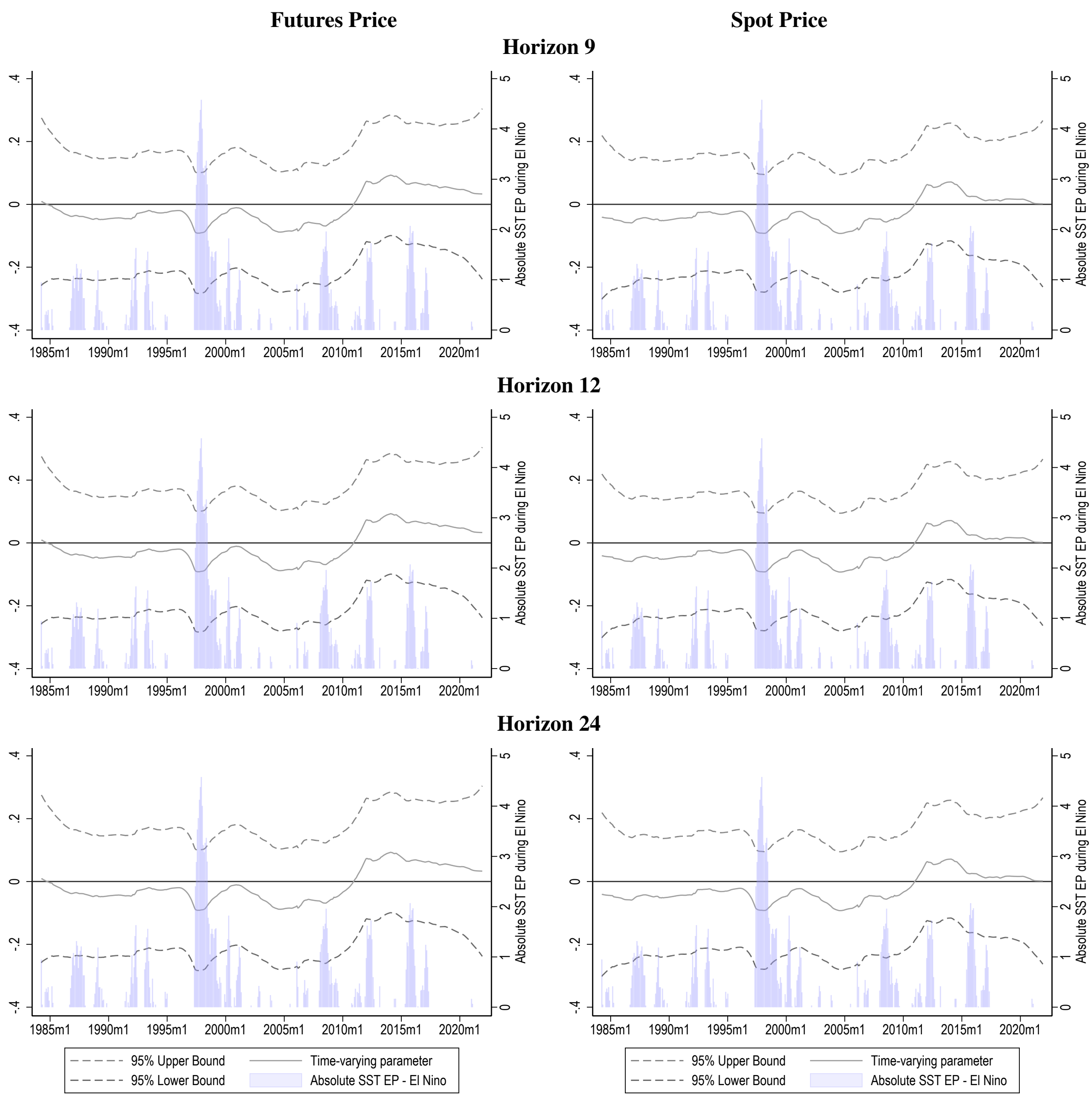

Note: Left (right) axis refers to IRFs (absolute SST during El Niño).

Figures A.11 and A.12 report the EP La Niña TVP-LP responses.

Figure A.11: Oil Price Reaction to La Niña Across Time (EP ENSO)

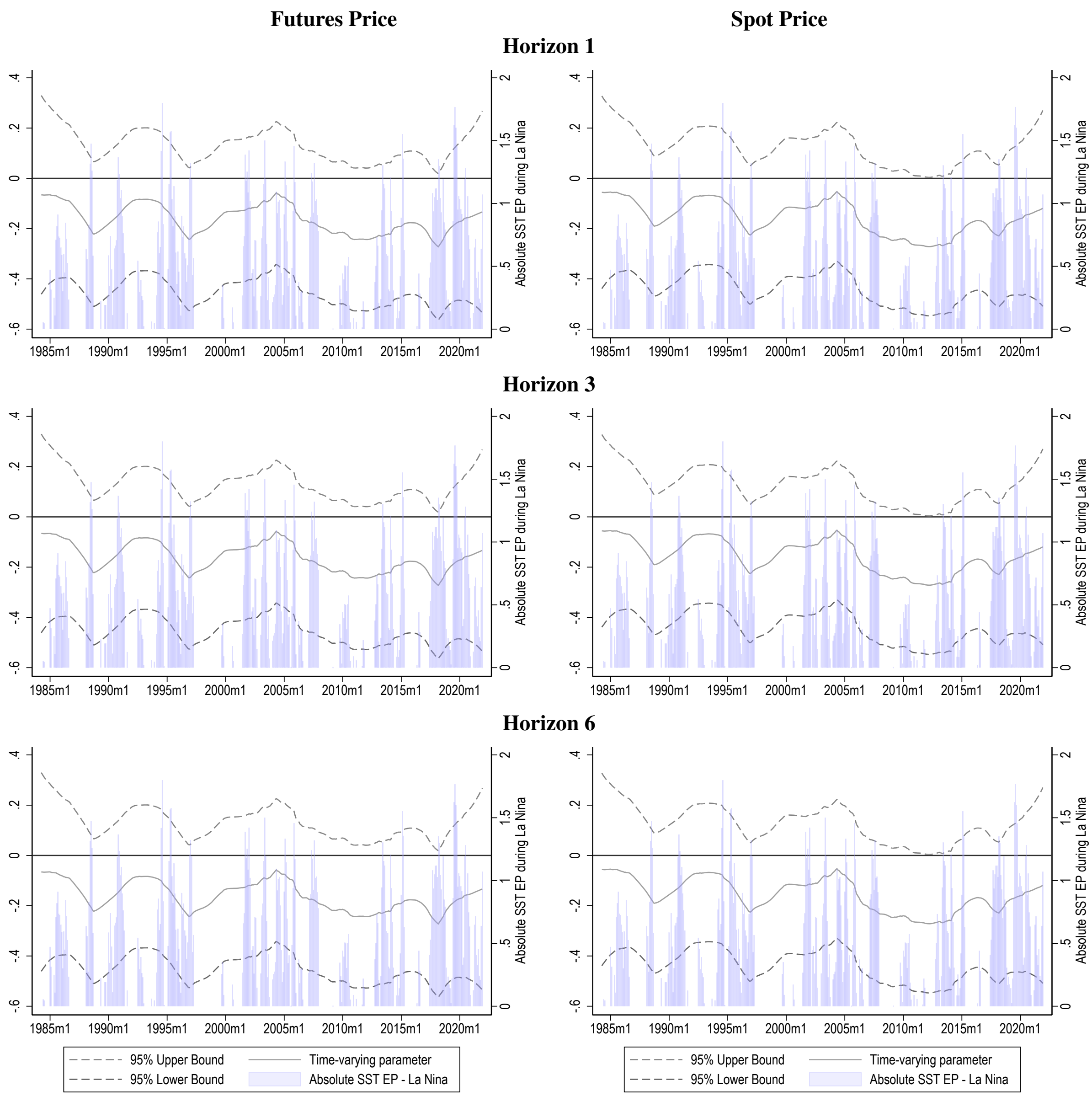

Note: Left (right) axis refers to IRFs (absolute SST during La Niña).

Figure A.12: Oil Price Reaction to La Niña Across Time (EP ENSO) (continued)

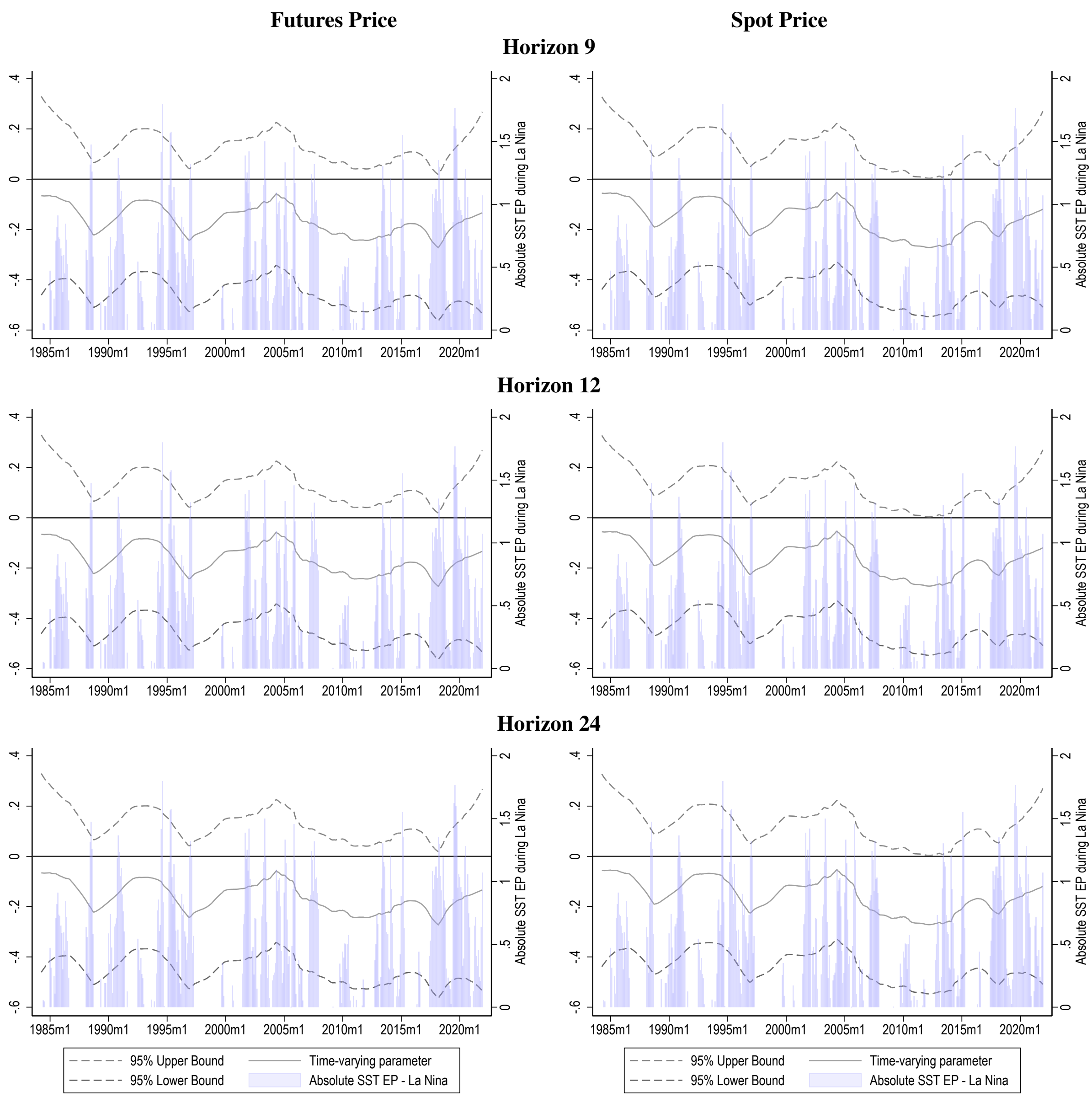

Note: Left (right) axis refers to IRFs (absolute SST during La Niña).

Figures A.13 and A.14 summarize the EP ENSO TVP-LP responses for futures and spot prices, including high-intensity ENSO events.

Figure A.13: Oil Futures Price Reaction to EP ENSO (TVP-LP)

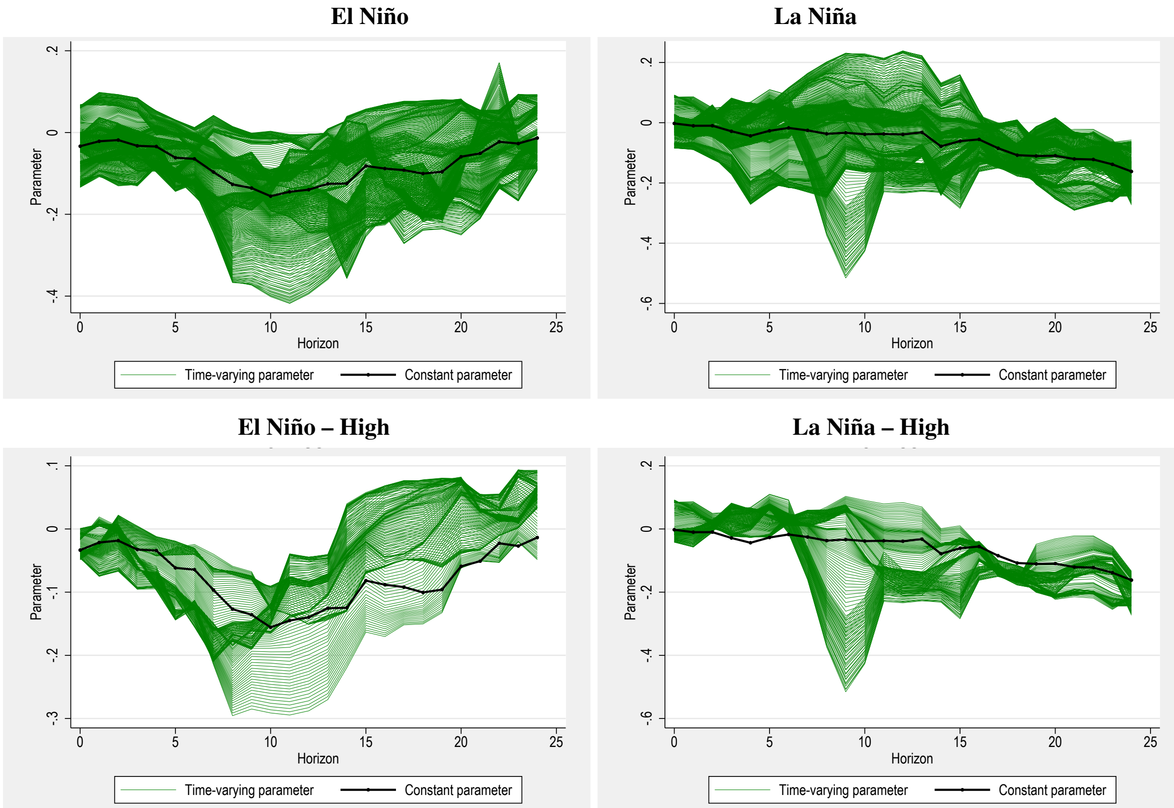

Note: "High" refers to anomalous El Niño and La Niña events defined as the top quartile (highest 25%) of the historical phase-specific anomaly distribution.

Figure A.14: Oil Spot Price Reaction to EP ENSO (TVP-LP)

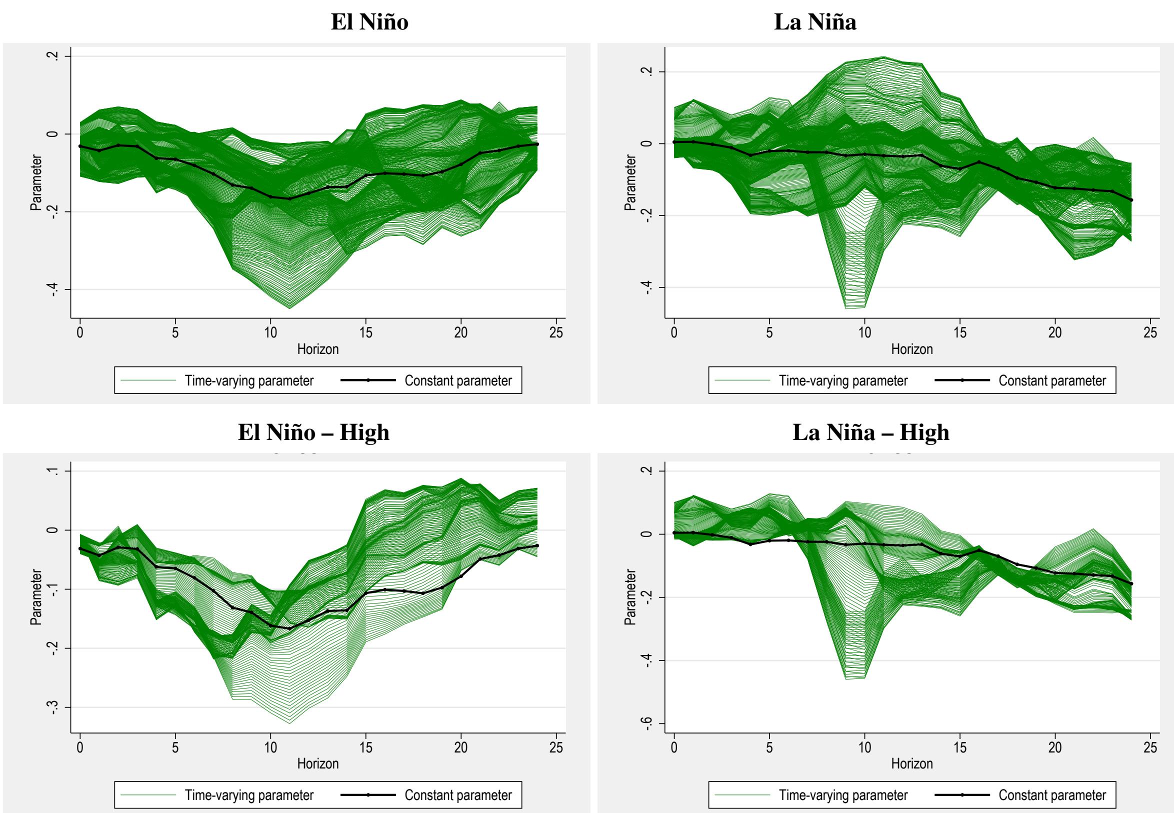

Note: "High" refers to anomalous El Niño and La Niña events defined as the top quartile (highest 25%) of the historical phase-specific anomaly distribution.